ANNUAL REVIEWS

Annual Review of Biochemistry

$PI(4,5)P_2$ Clustering and Its Impact on Biological Functions

Yi Wen, Volker M. Vogt, and Gerald W. Feigenson

Department of Molecular Biology and Genetics, Cornell University, Ithaca, New York 14850, USA; email: yw592@cornell.edu, vmv1@cornell.edu, gwf3@cornell.edu

Annu. Rev. Biochem. 2021. 90:681–707

First published as a Review in Advance on January 13, 2021

The *Annual Review of Biochemistry* is online at biochem.annualreviews.org

https://doi.org/10.1146/annurev-biochem-070920-094827

Keywords

phosphatidylinositol 4,5-bisphosphate, $PI(4,5)P_2$, cluster, multivalent cations, viral proteins, plasma membrane

Abstract

Located at the inner leaflet of the plasma membrane (PM), phosphatidylinositol 4,5-bisphosphate [$PI(4,5)P_2$] composes only 1–2 mol% of total PM lipids. With its synthesis and turnover both spatially and temporally regulated, $PI(4,5)P_2$ recruits and interacts with hundreds of cellular proteins to support a broad spectrum of cellular functions. Several factors contribute to the versatile and dynamic distribution of $PI(4,5)P_2$ in membranes. Physiological multivalent cations such as Ca^{2+} and Mg^{2+} can bridge between $PI(4,5)P_2$ headgroups, forming nanoscopic $PI(4,5)P_2$–cation clusters. The distinct lipid environment surrounding $PI(4,5)P_2$ affects the degree of $PI(4,5)P_2$ clustering. In addition, diverse cellular proteins interacting with $PI(4,5)P_2$ can further regulate $PI(4,5)P_2$ lateral distribution and accessibility. This review summarizes the current understanding of $PI(4,5)P_2$ behavior in both cells and model membranes, with emphasis on both multivalent cation– and protein-induced $PI(4,5)P_2$ clustering. Understanding the nature of spatially separated pools of $PI(4,5)P_2$ is fundamental to cell biology.

Contents

1. PHOSPHOINOSITIDES

Phosphoinositides (PIPs) are phosphorylated derivatives of phosphatidylinositol (PI) in cells. Since the discovery of PI/PIP signaling cycles by Mabel and Lowell Hokin in the 1950s (1), these lipids have gained significant research interest because they profoundly affect hundreds of biochemical processes in eukaryotic cells. PI is synthesized primarily in the endoplasmic reticulum (ER) and is then transferred to other membranes either by vesicular transport or by nonvesicular lipid transport via PI transfer proteins (PITPs) (2). PITPs sequester PI from a membrane in a hydrophobic pocket and deliver it to specific membrane compartments for further phosphorylation by numerous lipid kinases, which makes PITPs critical regulators of PIP pathways (3, 4). Reversible phosphorylation of the PI inositol ring at positions 3, 4, and 5 produces seven PIP species. Each PIP is predominantly found at a distinct subcellular location (**Figure 1**). Their spatial distribution, steady-state levels, and conversion to other species are primarily regulated by PIP kinases and phosphatases, whose localization and activation are also tightly controlled (5). Among PIPs, phosphatidylinositol 4,5-bisphosphate [$PI(4,5)P_2$] is the most abundant PIP found in mammalian cells. $PI(4,5)P_2$ plays critical roles in cell life and death, and many aspects of $PI(4,5)P_2$ biology have been intensively reviewed (6–13). The in vivo effects of $PI(4,5)P_2$ are complicated to work out because hundreds of proteins bind to it. In addition, $PI(4,5)P_2$ itself is an unusual phospholipid with unique properties that complicate its biochemistry, and these complexities likely affect its behavior in cells, even independently of protein binding. This review focuses on the biochemical and biophysical properties of $PI(4,5)P_2$ and highlights its unique clustering properties and its effects on biological functions.

2. $PI(4,5)P_2$ HEADGROUPS AND ACYL CHAINS

$PI(4,5)P_2$ is among the most highly charged anionic phospholipids, and it exhibits rich physical chemistry. $PI(4,5)P_2$ contains two phosphomonoesters at positions 4 and 5 and one

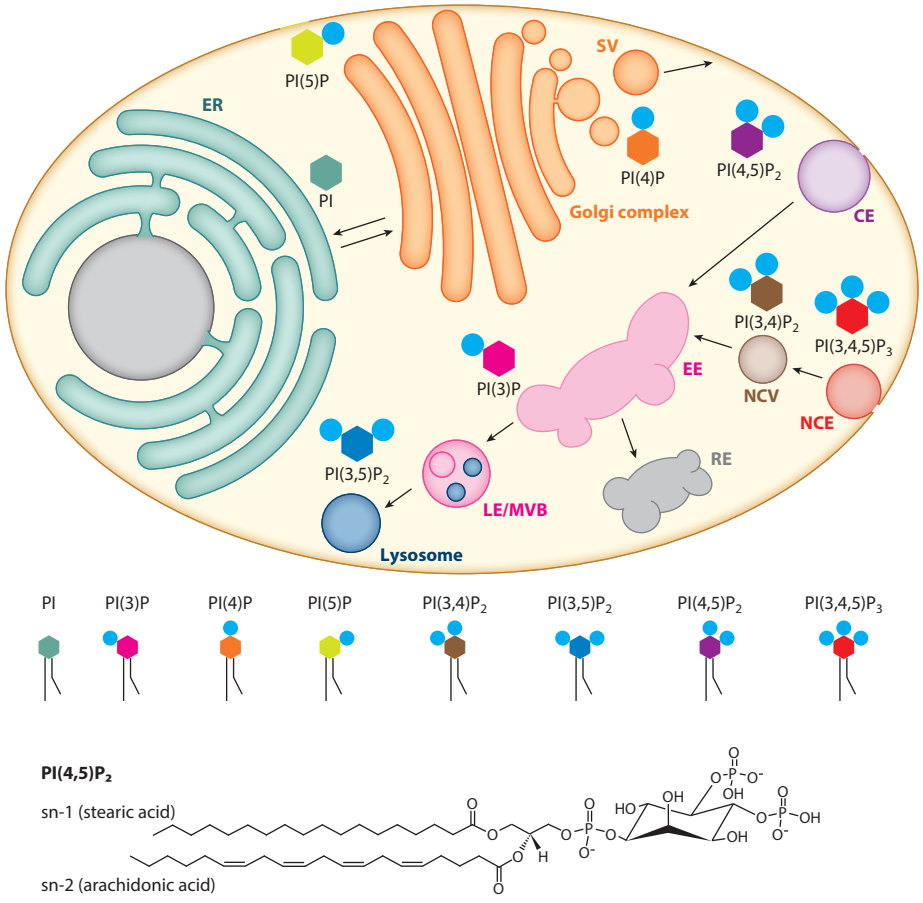

Figure 1

Subcellular distributions of PI and PIPs. The headgroup of each PIP is simplified as an inositol ring with 1–3 phosphate groups at different positions. This depiction is a simplification, illustrating only the most prominent location where each phosphoinositide species is found. Black arrows indicate the progression of the membrane trafficking pathway. The $PI(4,5)P_2$ structure is shown at the bottom. $PI(4,5)P_2$ containing stearic acid (18:0) on sn-1 and arachidonic acid (20:4) on sn-2 is the predominant species of natural $PI(4,5)P_2$. Abbreviations: CE, clathrin-dependent endocytosis; EE, early endosome; ER, endoplasmic reticulum; LE, late endosome; MVB, multivesicular body; NCE, nonclathrin endocytosis; NCV, nonclathrin endocytic vesicle; PI, phosphatidylinositol; PIP, phosphoinositides; RE, recycling endosome; SV, secretory vesicle.

phosphodiester at position 1 that connects the headgroup to the glycerol backbone (**Figure 1**). The ionization behavior of $PI(4,5)P_2$ has been studied extensively using ^{31}P-nuclear magnetic resonance (NMR) (14–19). In micelles and bilayers, the charge of $PI(4,5)P_2$ was estimated based on the phosphorus chemical shift at different pH values (20, 21). To determine the contribution to the membrane charge from anionic lipids such as PIPs, it is important to know their intrinsic pK_a (22). The pK_as of the 4-phosphate and 5-phosphate were found to be 6.7 and 7.7, respectively, resulting in an overall charge of approximately −4 at a physiological pH of 7.2 (14). However, $PI(4,5)P_2$ in bilayers has a net charge of approximately −3 at the physiological ionic strength of 100 mM KCl at pH 7.0 according to electrophoretic mobility assays. This decreased charge per membrane-bound $PI(4,5)P_2$ is caused by the abundant phosphatidylserine (PS) in physiological

membranes, which renders the overall membrane surface charge negative, making the creation of additional negative charge from $PI(4,5)P_2$ headgroup ionization less favorable (21, 23). Electrostatic effects, including the electric field differences between $PI(4,5)P_2$ and PS, have been explored by McLaughlin et al. (10). PS and $PI(4,5)P_2$ can attract proteins with basic patches in a distinct manner and sometimes in a synergistic manner (24). Upon protein binding or during Ca^{2+} or Zn^{2+} transient influx, the proton bound to $PI(4,5)P_2$ might also be displaced; thus, the net charge of $PI(4,5)P_2$ could be -3, -4, or -5. Different ionization properties of the phosphomonoesters allow $PI(4,5)P_2$ to form both intramolecular hydrogen bonds with adjacent hydroxyl groups and intermolecular hydrogen bonds with neighboring $PI(4,5)P_2$ molecules (14, 15, 17–19).

Natural $PI(4,5)P_2$ has a mixture of different acyl chains, with the predominant species being sn-1 stearoyl and sn-2 arachidonoyl (25). The two acyl chains attached to the first and second carbons of the glycerol are denoted as sn-1 and sn-2, respectively. The saturated stearoyl chain is 18 carbons long, while the polyunsaturated arachidonoyl chain is 20 carbons long with four double bonds. This high degree of unsaturation makes $PI(4,5)P_2$ prefer a disordered environment (26). However, $PI(4,5)P_2$ has also been reported to be associated with membrane regions known as rafts or detergent-resistant membranes (10, 13, 27, 28), which are enriched in cholesterol and saturated phospholipids with a higher degree of membrane order than other membrane regions (29, 30). The association between $PI(4,5)P_2$ and the lipid rafts is a puzzling observation, because rafts are a property of the coexisting phases in the outer leaflet of the plasma membrane (PM), whereas $PI(4,5)P_2$ is exclusively located at the inner PM leaflet. A plausible explanation, but one not yet supported by experiments, is that the inner leaflet $PI(4,5)P_2$ is located preferentially across the PM from an outer leaflet raft, leading to the cytosolic $PI(4,5)P_2$-binding proteins being identified as raft markers (31).

3. $PI(4,5)P_2$ FUNCTION IN CELLS

$PI(4,5)P_2$ composes approximately 1–2 mol% of total PM lipids, corresponding to 10,000–20,000 molecules/μm^2 at the inner leaflet where it is found (32). In a crude model of all phospholipids being dissolved in the cytoplasm, the effective concentration of $PI(4,5)P_2$ in the cell was calculated to be approximately 10 μM (10). The synthesis of $PI(4,5)P_2$ is primarily mediated by the PIP kinases phosphatidylinositol 4-phosphate 5-kinase (PIP5K), which phosphorylates PI(4)P, or to a lesser extent, phosphatidylinositol 5-phosphate 4-kinase (PIP4K), which phosphorylates PI(5)P (33). $PI(4,5)P_2$ is critically involved in different signal transduction pathways that regulate a broad spectrum of biological activities. $PI(4,5)P_2$ itself can act directly as a messenger (34) or serve as a precursor in the generation of the important secondary messengers inositol trisphosphate (IP3) and diacylglycerol (DAG), which are produced when $PI(4,5)P_2$ is hydrolyzed by phospholipase C (PLC) upon receptor stimulation (35). The rapid recovery of $PI(4,5)P_2$ levels at the PM following receptor-induced hydrolysis suggests a feedback loop of $PI(4,5)P_2$ consumption and replenishment to ensure cell homeostasis and signaling. Several proteins, such as Nir2, E-Syt1, and STIM1, which are localized to ER-PM junctions, have been reported to replenish $PI(4,5)P_2$ at the PM and Ca^{2+} in the ER following receptor-induced cell signaling (36). Phosphatidylinositol 3,4,5-trisphosphate [$PI(3,4,5)P_3$], which is involved in cell survival, cell growth, intracellular vesicle trafficking, cytoskeletal rearrangement, and cell metabolism, is generated from $PI(4,5)P_2$ by class I phosphoinositide 3-kinases (PI3Ks) (37). Even though the majority of $PI(4,5)P_2$ is located at the PM, a substantial pool of $PI(4,5)P_2$ is also found in the nucleus. Nuclear $PI(4,5)P_2$ is proposed to be located within nonmembrane structures, stabilizing nuclear $PI(4,5)P_2$-binding proteins, thereby contributing to nuclear $PI(4,5)P_2$ signaling (38). $PI(4,5)P_2$ also plays central roles in a broad spectrum of cellular functions, including exocytosis and endocytosis (8, 39), ion channel

and transporter regulation (40, 41), actin cytoskeleton assembly (42), endosomal trafficking (43, 44), membrane fusion (45), cell polarization (46), phagocytosis (47), and cell directional migration (48). $PI(4,5)P_2$ downstream signaling and $PI(4,5)P_2$-derived metabolites have been implicated in human diseases such as diabetes, bipolar disorder, and cancer (49, 50).

With its turnover being spatially and temporally regulated, $PI(4,5)P_2$ is well suited to recruit diverse cellular proteins and to interact with various effector proteins. Typically, $PI(4,5)P_2$-binding proteins are classified by function into several major categories, including membrane transport and trafficking, actin cytoskeletal dynamics and organization, functional enzymes, PM binding, small GTPase guanine nucleotide exchange factors and GTPase-activating proteins, and protein kinases and phosphatases, and several minor categories, including cell adhesion molecules, transcription and translation factors, and microtubule proteins (51).

A large group of $PI(4,5)P_2$-binding proteins is involved in membrane transport and trafficking. Endocytosis is regulated by $PI(4,5)P_2$ at several steps including vesicle formation, maturation, and fission. Clathrin-mediated endocytosis (CME) is a well-studied form of endocytosis that involves numerous proteins interacting with $PI(4,5)P_2$ using different strategies (52). The pleckstrin homology (PH) domain in dynamin-1 and -2, the ENTH (Epsin N-terminal homology) domain of Epsin1 and 2, the Hip1/1R domain, and the ANTH (AP180 N-terminal homology) domain of AP180 and CALM interact with $PI(4,5)P_2$ at defined binding sites. The α and $\mu 2$ subunits of AP-2, profilin, and the Wiskott-Aldrich Syndrome protein (WASP) family (44) bind to $PI(4,5)P_2$ via surface-exposed basic patches. Other actin-associated proteins, such as Bin-Amphiphysin-Rvs (BAR)-domain proteins that deform membranes, inducing protrusions or invaginations, interact with $PI(4,5)P_2$ headgroups electrostatically and cooperatively (53). Some BAR proteins insert amphipathic α-helices into the lipid bilayer. Other proteins that are involved in exocytosis associate with $PI(4,5)P_2$, including synaptotagmin-1, syntaxin-1A, Munc13, Rabphilin, VAMP-2, and granuphilin (9).

$PI(4,5)P_2$ is the best-characterized actin cytoskeleton regulator among all PIPs. $PI(4,5)P_2$ has been shown to facilitate actin cytoskeleton formation beneath the PM, and any change in $PI(4,5)P_2$ local concentrations affects actin dynamics. An increase in $PI(4,5)P_2$ levels activates proteins that induce actin filament assembly, such as ezrin, radixin, and moesin (ERM) family proteins, talin, and WASP family proteins that activate the Arp2/3 complex (42, 54). An increase in $PI(4,5)P_2$ levels also inhibits proteins that promote actin filament disassembly, such as gelsolin, heterodimeric capping protein, ADF/cofilin, profilin, and twinfilin (54). Actin and cytoskeletal modulating proteins use either defined $PI(4,5)P_2$-binding domains or a cluster of positively charged and/or hydrophobic residues such as MARCKS (myristoylated alanine-rich C kinase substrate), GAP43 (growth-associated protein of 43 kDa), and CAP23 (cortical-associated protein of 23 kDa, a cytoskeleton-associated protein). Furthermore, a number of actin-associated proteins, such as BAR-domain proteins, are capable of directly deforming PIP-rich membranes to induce PM protrusions or invaginations (53). A cluster of proteins targeted to the PM by $PI(4,5)P_2$ are classified as small GTPases or GTPase regulators, such as members of the Rho, Arf, Ras, and Rab families. These proteins usually harbor a polybasic patch and hydrophobic modifications such as palmitoyl, prenyl, or myristoyl. Proteins in the Rho and Arf6 families bind to $PI(4,5)P_2$ during cytoskeleton regulation (51).

$PI(4,5)P_2$ interacts directly with a variety of structured protein modules such as PH domains (55). PH domains, approximately 120 amino acids long, are best known for their ability to bind PIPs with high affinity and specificity, although less than 10% of all PH domains share this property (56). Most PH domains bind to $PI(4,5)P_2$ weakly and nonspecifically. Many PH domains share similar core structures consisting of a pair of antiparallel β-sheets with a C-terminal α-helix. There are three primary types of PIP-binding sites in PH domains: those that contain the $KX_n(K/R)XR$

motif or a canonical PIP-binding site in the loop connecting strands β1 and β2, such as a phospholipase Cδ1 PH domain (PH-PLCδ1) (57, 58); those that do not harbor the $KX_n(K/R)XR$ motif and instead have a noncanonical PIP-binding site, as found in the β-spectrin PH domain (59); and those that contain both canonical and noncanonical PIP-binding sites, such as the ASAP1 PH domain (60, 61). PH-PLCδ1 is the best characterized of the $PI(4,5)P_2$-specific binding proteins, and its fluorescent chimeric versions have been used to study cellular $PI(4,5)P_2$ localization and function (62, 63). Several basic residues in PH-PLCδ1 were predicted to bind to $PI(4,5)P_2$ (64). To test whether these basic residues are sufficient for specific $PI(4,5)P_2$ binding, a short peptide with amino acids corresponding to residues 30–43 of PH-PLCδ1 was synthesized; however, this peptide bound to $PI(4,5)P_2$ only weakly and exhibited little specificity (64). These observations suggest that the intact tertiary structure of the PH domain is required for high-affinity $PI(4,5)P_2$-specific interaction. The formation of hydrogen bonding networks between 4- and 5-position phosphates and lysine (Lys)30 and Lys57 in PH-PLCδ1 locks $PI(4,5)P_2$ inside of the binding pocket (57). PH-PLCδ1 is reported to bind to the $PI(4,5)P_2$ polar headgroup with a 1:1 stoichiometry and a K_d of 2 μM in vitro (65). Additionally, PH-PLCδ1 also binds to the soluble D-myo-IP3 with even higher affinity, almost eightfold greater than its affinity for $PI(4,5)P_2$ (57). Excess IP3 can abolish the binding of the PH domain to $PI(4,5)P_2$ in vitro, which would interfere with the function of the PH domain as a $PI(4,5)P_2$ sensor in cells.

FERM domains, which are approximately 300 amino acids in length, were originally defined by their presence at the N terminus of the erythrocyte band 4.1 protein (F) and the related cytoskeletal proteins ezrin (E), radixin (R), and moesin (M) (66). These domains are also found in the cytoskeletal protein talin, the tumor suppressor merlin, and several tyrosine kinases (such as JAK and FAK) and phosphatases (such as PTPN3 and PTPN4) (67). Upon binding to $PI(4,5)P_2$, the FERM domain of these proteins is released from its autoinhibitory state, allowing these proteins to serve as adaptors between the actin cytoskeleton and the PM (68). The FERM domain is composed of three subdomains, A, B, and C. Subdomain C contains a fold resembling a PH domain (69). However, the region responsible for $PI(4,5)P_2$ binding is a basic cleft between subdomains A and C. Further mutagenesis studies imply that other regions of the FERM domain may also contribute to $PI(4,5)P_2$ binding. The residues involved in $PI(4,5)P_2$ binding are conserved, and the sequence homology suggests they form a potential $PI(4,5)P_2$-binding pocket.

Another $PI(4,5)P_2$-binding module is the ENTH domain, which plays a critical role in CME (70). ENTH domains contain approximately 140 amino acids and are found in Epsin1 and 2 and Hip1R. NMR studies determined that positively charged residues in a cleft of the epsin ENTH domain contribute to $PI(4,5)P_2$ binding (71). ENTH binds to $PI(4,5)P_2$ much more strongly than a related domain called ANTH does. Another structured domain selectively binding to $PI(4,5)P_2$ is the PX domain of the CPK PI3K (70).

While many proteins have developed specific $PI(4,5)P_2$-binding pockets, other proteins use unstructured basic regions to bind to $PI(4,5)P_2$ via nonspecific electrostatic interactions. The MARCKS protein is among the best studied of these (10, 72). MARCKS protein binds to the negatively charged inner leaflet of the PM using two mechanisms: An N-terminal myristate inserts hydrophobically into the bilayer, and a conserved effector domain interacts with the membrane via its 13 basic residues (residues 151–175: KKKKKRFSFKKSFKLSGFSFKKNKK). The MARCKS effector domain binds to and sequesters three $PI(4,5)P_2$ molecules (10, 73). The five aromatic phenylalanine residues in the effector domain were shown to be inserted into bilayers (74–76). This insertion pulls the adjacent basic residues closer to the membrane surface where the electrostatic potential is stronger, thereby enhancing lateral $PI(4,5)P_2$ sequestration. Membrane-bound MARCKS can be dissociated from the PM by Ca^{2+}-loaded calmodulin or by phosphorylation of the Ser residues of the effector domain by protein kinase C (PKC) (10).

Treating these membrane-bound molecules simplistically, as if they were water-soluble molecules within the volume of the cytosol, the physiological level of MARCKS is estimated to be ~2 μM in fibroblasts and ~10 μM in neuronal tissue, a range similar to that estimated for $PI(4,5)P_2$ in cells (10). Thus, MARCKS could potentially bind and sequester a significant fraction of cellular $PI(4,5)P_2$. MARCKS-sequestered $PI(4,5)P_2$ would be less susceptible to hydrolysis by PLCδ1 compared with exposed $PI(4,5)P_2$ when MARCKS is dissociated. In addition to MARCKS, $PI(4,5)P_2$ binds strongly to GAP43 and CAP23 (26). These three motility-associated proteins are termed GMC proteins, and they share important properties: They all contain a basic effector domain, are reported to localize in the cholesterol-enriched domains termed rafts, and laterally sequester $PI(4,5)P_2$ (77). The association between GAP43 and rafts was found to require dual palmitoylation of its N terminus (78).

4. ROLE OF $PI(4,5)P_2$ IN VIRUS REPLICATION

Besides the numerous roles $PI(4,5)P_2$ plays in maintaining normal cell functions, it is also indispensable during the life cycle of many viruses, including human immunodeficiency virus 1 (HIV-1) and Ebola virus. Consistent with its roles in vesicle transport, trafficking, and actin cytoskeletal regulation, $PI(4,5)P_2$ also affects viruses that hijack cellular machinery during various stages of infection.

The role of $PI(4,5)P_2$ begins as early as viral entry. Many enveloped viruses such as influenza virus and vesicular stomatitis virus use $PI(4,5)P_2$-dependent CME for productive infection (79, 80). Some nonenveloped viruses that use integrins as their receptors, such as foot-and-mouth disease virus, also are highly dependent on $PI(4,5)P_2$ for internalization (81). One study (82) reported that $PI(4,5)P_2$ plays a role in HIV-1 entry.

$PI(4,5)P_2$ is essential for the genome replication of some viruses, such as hepatitis C virus (HCV). HCV, like other flaviviruses, replicates its RNA genome in close contact with invaginated membranous structures that might be derived from organelles such as the ER, Golgi complex, and endosomes (83). The N-terminal amphipathic helix (AH) of the nonstructural protein NS5A binds to $PI(4,5)P_2$ through a pair of highly conserved basic amino acids, Lys20 and Lys26. This NS5A–$PI(4,5)P_2$ interaction induces a conformational change that stabilizes the interaction between NS5A and TBC1D20, a GTPase-activating protein for Rab1, which is required to establish efficient HCV replication (84). Importantly, these Lys residues are highly conserved across all HCV isolates and the NS4B protein of the distantly related polioviruses and rhinoviruses.

The most studied role of $PI(4,5)P_2$ during the viral life cycle is in viral assembly (85). Many cell studies have shown that $PI(4,5)P_2$ is critical for HIV-1 particle assembly (86, 87). The HIV-1 structural protein, Gag, is the primary driving force of viral assembly on membranes. Depleting $PI(4,5)P_2$ at the PM by overexpressing 5-phosphatase IV (5ptaseIV), which breaks down $PI(4,5)P_2$, significantly reduces both HIV-1 assembly at the PM and viral release from cells. Altering the localization of $PI(4,5)P_2$ to endosomal compartments by expressing an Arf6 mutant, Q67L, also drastically reduces virus release from cells (86). A recent study with living cells observed less HIV-1 Gag assembly following rapid $PI(4,5)P_2$ depletion at the PM and enhanced Gag assembly upon restoration of PM $PI(4,5)P_2$ levels (88). Similarly, several biochemical studies suggest that the membrane binding of HIV-1 Gag and Gag-related proteins is significantly enhanced in the presence of $PI(4,5)P_2$, as shown by both liposome flotation assays and pelleting assays (89, 90). All of these results suggest that basic residues in Matrix (MA), the membrane-binding domain of Gag, interact directly with $PI(4,5)P_2$. HIV-1 MA binds to membranes using a bipartite signal: The highly basic region binds to negatively charged lipids such as PS and $PI(4,5)P_2$ in membranes through electrostatic interaction, and the N-terminal myristate moiety inserts into the membrane core

through hydrophobic interactions. Specific HIV-1 MA interactions with $PI(4,5)P_2$ were detected by mass spectrometric protein footprinting (91). NMR studies also confirmed that the HIV-1 MA domain binds specifically to water-soluble short-chain (C4 and C8) analogs of $PI(4,5)P_2$ (91). Lipidomic studies suggest that HIV-1 virions have an elevated $PI(4,5)P_2$ level compared with the host PM from which the virions bud (92, 93). This $PI(4,5)P_2$ enrichment requires the HIV-1 MA domain; a Gag mutant lacking the polybasic globular head of MA but still containing the N-terminal myristate incorporates significantly less $PI(4,5)P_2$ than the wild type (94). HIV-1 viral membranes were also reported to have increased levels of the raft lipid components cholesterol and sphingomyelin, as well as lipids from the cytosolic leaflet, such as $PI(4,5)P_2$, PS, and plasmalogen-phosphatidylethanolamine (92–95). It was therefore hypothesized that HIV-1 buds from $PI(4,5)P_2$-rich raft-like microdomains and that HIV-1 exploits MA–$PI(4,5)P_2$ interactions for efficient virus assembly and release.

MA interaction with $PI(4,5)P_2$ has also been reported for other retroviruses, such as HIV-2, Mason-Pfizer monkey virus, equine infectious anemia virus, and murine leukemia virus (96–98). In contrast, human T-lymphotropic virus type 1 (99) and Rous sarcoma virus (RSV) (100) are reported to be much less dependent on $PI(4,5)P_2$ for viral assembly and release than HIV-1 Gag. In addition to retroviruses, several studies show that $PI(4,5)P_2$ is required to stabilize and/or induce oligomerization of the Ebola virus (a filovirus) structural protein VP40 at the PM. VP40 has been shown to be indispensable for viral particle formation (101). However, the VP40 of another filovirus, Marburg virus, seems to lack specific interactions with $PI(4,5)P_2$, instead acting as a promiscuous anionic charge sensor (102). A recent study suggests that influenza hemagglutinin (HA) protein tightly colocalizes with $PI(4,5)P_2$ at the PM in infected cells (103).

In addition to transmission through the release of viral particles into the extracellular space, viruses like HIV-1 can also be spread through cell–cell transmission by forming a virological synapse (VS) (104). A VS forms at the contact site of infected and uninfected T cells, mediated by envelope glycoprotein interactions with their receptor (CD4) and coreceptors (CXCR4 and CCR5) (105). Synapse complex formation relies on efficient actin cytoskeleton remodeling in the target cells (106). Upon Env and Gag recruitment to the cell–cell contact sites, viral particles transfer across the VS into the uninfected cells. $PI(4,5)P_2$ is involved in this process, since it regulates actin-binding protein accumulation that triggers VS formation, thus ensuring efficient viral dissemination.

5. $PI(4,5)P_2$ MICELLE FORMATION

The amphipathic nature of $PI(4,5)P_2$ results in two major forms of aggregation in the presence of water: micelles and membrane bilayers. These self-assemblies of phospholipids are driven by increased water entropy when the nonpolar tails are removed from water and are stabilized by electrostatic and hydrogen bond interactions among hydrophilic heads, cations, and the aqueous environment. Other phospholipids with long acyl chains form bilayers, but micelles are not detected because of extreme insolubility. The strongly hydrophilic headgroup makes $PI(4,5)P_2$ capable of forming micelles in an aqueous environment (107, 108), but in the presence of sufficient bilayer phase, $PI(4,5)P_2$ is more stable partitioning into the lipid bilayers.

A characteristic of any micelle-forming surfactant is the critical micelle concentration (CMC) (109), defined as the concentration above which surfactant monomers aggregate to form micelles. Beyond the CMC, any additional surfactant of the same type forms more micelles, leaving the monomer concentration almost constant. The shape and size of a micelle are dependent on the molecular structure and the aqueous conditions such as surfactant concentration, pH, ionic type and strength, and temperature. Among common methods to determine CMC are light scattering,

dye solubilization, and surface tension (109). Both light scattering and the solubility of a hydrophobic dye increase abruptly with increasing surfactant concentration above the CMC, whereas surface tension decreases with increasing surfactant monomer concentration, reaching a minimum value at the CMC. A few measurements of CMC values for $PI(4,5)P_2$ have been reported, for example, a CMC of 30–40 μM using light scattering (110), a CMC of 10 μM using a Coomassie blue dye method (111), and a CMC of 12.5 μM using the fluorescent dye DPH (112). Additionally, one group observed that the $PI(4,5)P_2$ CMC in the buffers 50 mM PIPES and 50 mM Tris at pH 7.0 is 30 μM, whereas that in water is 200 μM (113). Our data (Y. Wen, A. Matsumoto & G.W. Feigenson, unpublished data) suggest that the CMC of the natural brain $PI(4,5)P_2$ is approximately 0.5 μM in a buffer of 100 mM KCl, 20 mM HEPES, pH = 7.2, as measured by light scattering. We also found that the $PI(4,5)P_2$ CMC is lower in the presence of multivalent cations than in the presence of EDTA.

The aggregation number of each $PI(4,5)P_2$ micelle has been reported by gel filtration chromatography of the $PI(4,5)P_2$ micelle in complex with $PI(4,5)P_2$-binding proteins, such as PKC or profilin (114, 115). These complexes form micelles of molecular weight 93,000 with an estimated aggregation number of 82 and a Stokes radius of 39 Å. Interestingly, Janmey and colleagues (116, 117) showed that $PI(4,5)P_2$ exists as small micelles in the presence of buffer ions and/or monovalent cations, such as 100 mM NaCl or KCl, whereas the addition of millimolar concentrations of divalent cations such as Mg^{2+}, Ca^{2+}, or Ba^{2+} induces the formation of large, multilamellar $PI(4,5)P_2$ aggregates that are visible by electron microscopy (EM). This $PI(4,5)P_2$ cluster formation with divalent cations presumably occurs through bridging of $PI(4,5)P_2$ headgroups. The addition of EDTA or EGTA disrupts these $PI(4,5)P_2$ aggregates, confirming that this process is reversible. In summary, the formation of $PI(4,5)P_2$ aqueous micelles can be thought of as the form of $PI(4,5)P_2$ clustering behavior in the absence of bilayers. Even though this type of clustering as micelles is probably not physiologically relevant, it does indicate how interactive $PI(4,5)P_2$ headgroups are with each other, despite multiple negative charges.

6. $PI(4,5)P_2$ CLUSTERING BEHAVIOR IN VIVO

Evidence suggests that $PI(4,5)P_2$ forms clusters in the cellular PM. The Fujimoto group (118) visualized concentrated $PI(4,5)P_2$ pools at the rims of caveolae as well as in coated pits in cultured cells using an EM technique. Live cells were rapidly frozen without chemical fixation, and $PI(4,5)P_2$ was labeled with a GST-tagged PH-PLCδ1 probe. Caveolin-1 and caveolin-2 sequester $PI(4,5)P_2$ electrostatically, and these proteins assemble into heterooligomers to generate the caveolae with locally concentrated $PI(4,5)P_2$. Many studies report $PI(4,5)P_2$ clustering in intact cells or on membrane sheets derived from cells, and most of these studies detect $PI(4,5)P_2$ accumulation with fluorescently labeled PH-PLCδ1, acyl-chain-labeled fluorescent $PI(4,5)P_2$, or $PI(4,5)P_2$-specific antibodies. Many groups have used superresolution microscopy to visualize $PI(4,5)P_2$. Using direct stochastic optical reconstruction microscopy (dSTORM) with $PI(4,5)P_2$-specific antibodies directly conjugated with Alexa Fluor 647, $PI(4,5)P_2$ clusters were found in domains of approximately 65 nm in intact PC12 cells (119). Three quarters of the observed $PI(4,5)P_2$ clusters were reported to be elongated and one quarter to be circular. A study using stimulated-emission depletion (STED) microscopy suggested that $PI(4,5)P_2$ composes approximately 80% of the inner leaflet lipids within clusters. These $PI(4,5)P_2$ clusters measured approximately 70 nm in diameter when detected with fluorescent PH-PLCδ1 or approximately 90 nm in diameter when detected with a $PI(4,5)P_2$ antibody, which indicates that approximately 1,000 $PI(4,5)P_2$ molecules are present in each cluster (120). Another superresolution imaging study revealed that $PI(4,5)P_2$ distribution is homogenous in the majority of the PM by area, as detected by PH-PLCδ1. The authors

observed only some sparse PI(4,5)P_2-enriched regions with an average diameter of approximately 380 nm (121). Using fluorescence photoactivation localization microscopy (FPALM), a recent study showed that influenza HA protein coclusters with PI(4,5)P_2, with cluster diameters of approximately 135 nm and 182 nm with low and high influenza HA concentrations, respectively. Interestingly, the authors found that many PI(4,5)P_2 clusters are elongated instead of round and that PI(4,5)P_2-binding sites indicate a radial attractive gradient around the HA protein (103). Another experiment using FPALM with acyl-chain-labeled fluorescent PI(4,5)P_2 delivered across the PM by the carrier protein histone H1 also detected PI(4,5)P_2 clusters in live cells that were approximately 150 nm in diameter; even larger clusters are found in fixed cells, approximately 400 nm in diameter, when detected by fluorescent PH-PLCδ1. Of note, another group using confocal microscopy (122) reported that the size of the PI(4,5)P_2 clusters detected using a PI(4,5)P_2 secondary antibody was enhanced upon adding a tertiary antibody. Thus, the visualization of PI(4,5)P_2 clusters using antibodies needs to be carefully examined and interpreted.

Numerous cellular PI(4,5)P_2-binding proteins are also proposed to modulate PI(4,5)P_2 distribution and induce PI(4,5)P_2 cluster formation. For example, MARCKS, GAP43, CAP23, and syntaxin-1 have been reported to laterally sequester PI(4,5)P_2 at the PM (77, 123). A large fraction of PI(4,5)P_2 at the inner leaflet is believed to be electrostatically sequestered or bound to and released by proteins containing a basic patch, such as MARCKS protein (10). Each MARCKS protein can bind three PI(4,5)P_2 molecules with a dissociation constant of 10^{-8} M (105). This bound PI(4,5)P_2 is released only upon transient Ca^{2+} influx or upon phosphorylation of a key serine residue by PKC. At the same time, other effector proteins could have access to these concentrated PI(4,5)P_2 platforms to activate downstream functions. Only a small fraction of PI(4,5)P_2 is believed to diffuse freely in the PM. The evidence for PI(4,5)P_2 being laterally sequestered by proteins comes from cellular studies. In several cell types, MARCKS is not uniformly distributed at the PM but is enriched in membrane ruffles or nascent phagosomes (124, 125). A similar PI(4,5)P_2 distribution pattern was later observed using fluorescent PH-PLCδ probes (125). Importantly, van Rheenen et al. (126), using advanced imaging methods to characterize the bumpy cell surface, showed that the apparent enrichment of PI(4,5)P_2 detected by PH-PLCδ clustering was not due to PI(4,5)P_2 cluster formation but instead was caused by an increased lipid content in submicroscopic folds and ruffles and thus was a visualization artifact. When MARCKS was disassociated from the PM into the cytosol by PKC phosphorylation, the free PI(4,5)P_2 level at the PM increased as membrane tension increased due to PI(4,5)P_2-dependent cytoskeletal adhesion to the PM. Another study used antibody labeling to show that PI(4,5)P_2 colocalized with the GMC proteins MARCKS, GAP43, and CAP23 in cholesterol-rich microdomains in many cell lines (77). Overexpression of GMC increases the detectable PI(4,5)P_2 clusters; GMC lacking effector domains seems to reduce PI(4,5)P_2 accumulation. However, the characteristic patchy pattern of GMC and PI(4,5)P_2 microdomains was not detectable when macroscopic clusters of GPI-linked proteins were prevented from forming by fixation with glutaraldehyde (77).

Other groups used unfixed PC12 cell membrane sheets, derived from the PM by gentle sonication, to study PI(4,5)P_2 lateral organization (120, 123). They reported that syntaxin-1, a SNARE protein that catalyzes regulated exocytosis, forms clusters in the PM, mediated by electrostatic interactions with PI(4,5)P_2. Syntaxin-1 contains a transmembrane domain juxtaposed to a polybasic region (basic residues KARRKK), which sequesters PI(4,5)P_2 headgroups. Using STED, they found that the polybasic region is required for PI(4,5)P_2 coclustering with syntaxin-1 and that nanoscopic PI(4,5)P_2 clusters were also required for syntaxin-1 sequestering (120, 123). PI(4,5)P_2–syntaxin clusters serve as recognition and association sites for vesicle docking during Ca^{2+}-stimulated membrane fusion. Another group reported that Ca^{2+} links smaller PI(4,5)P_2–syntaxin-1 clusters into larger domains and that this clustering effect is reversible (127).

Locally concentrated $PI(4,5)P_2$–Ca^{2+} clusters can recruit more downstream effector proteins such as CAPS, Munc13, and synaptotagmin to facilitate assembly of the complete fusion machinery at the site of release (123). Together, these studies suggest that $PI(4,5)P_2$ clustering may occur as a consequence of lateral sequestration by effector proteins upon physiological Ca^{2+} influx and that these protein–$PI(4,5)P_2$ clusters regulate the accessibility of $PI(4,5)P_2$ to other effector proteins.

In addition to protein sequestration, upon activation of specific PIP kinases, $PI(4,5)P_2$ synthesis is localized to the inner leaflet of the PM (128). Type I PIP5K is mostly responsible for the generation of $PI(4,5)P_2$ from PI(4)P at the PM, since PI(4)P is the second most abundant PIP at the inner leaflet (7). Via distinct signaling pathways, PIP5K isoforms and splice variants have specific interactions with different proteins that allow PIP5K to target subcellular locations such as the PM, focal adhesions, the Golgi complex, and the nucleus (129). $PI(4,5)P_2$ is also locally synthesized at sites of actin remodeling, giving rise to membrane ruffles, filopodia, lamellipodia, and phagosomes. $PI(4,5)P_2$ accumulation at phagosomes due to PIP5K has been detected (43). This accumulation is transient, as the DAG level significantly increases and the $PI(4,5)P_2$ level decreases upon PLC activation. Small GTPases such as Rho, Rac family members, Arf6, specific proteins such as talin, and phospholipids such as phosphatidic acid (PA) have been shown to activate and regulate PIP5K activity and then modulate localized $PI(4,5)P_2$ synthesis (7, 9). Targeted $PI(4,5)P_2$ production by PIP5K further regulates various $PI(4,5)P_2$ effector proteins during biological functions. At a larger scale, compartmentalization in these small structures, such as in membrane protrusions of chemotactic and phagocytic cells, limits the rapid diffusion of locally generated $PI(4,5)P_2$ and can lead to a local $PI(4,5)P_2$ gradient (130). $PI(4,5)P_2$ gradients result from a combination of local synthesis, breakdown, and lipid lateral diffusion. Thus, it is likely that these separate $PI(4,5)P_2$ pools are spatially and temporally choreographed by a combination of enzymes, effector proteins, and probably other cytosolic factors (13). However, the mechanistic details of how the separate pools of $PI(4,5)P_2$ form are unclear, and in vitro studies could provide more information at a molecular level.

7. $PI(4,5)P_2$ CLUSTERING BEHAVIOR IN VITRO

Models of $PI(4,5)P_2$ accumulation in vitro are primarily based on mechanistic details of $PI(4,5)P_2$ cluster formation. Several models could explain $PI(4,5)P_2$ clustering in bilayers. $PI(4,5)P_2$ clustering is proposed to be induced by a combination of electrostatic bridging by multivalent cations such as Ca^{2+} and Mg^{2+} (**Figure 2**) (131–133), hydrogen bonding networks among $PI(4,5)P_2$ headgroups (10, 15, 17–19), and basic patches of proteins (74). Molecular dynamics simulations (134) indicate that clustered $PI(4,5)P_2$ affects protein binding, with protein binding further modulating $PI(4,5)P_2$ enrichment.

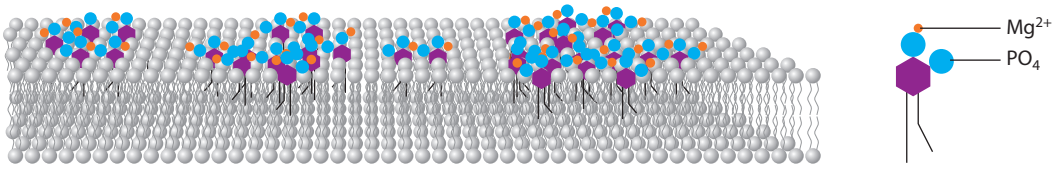

Figure 2

Schematic depiction of $PI(4,5)P_2$ clusters bridged by multivalent cations. Multivalent cations, such as Mg^{2+}, are shown as orange circles. Each $PI(4,5)P_2$ headgroup is shown as a purple inositol ring with two blue phosphate groups at positions 4 and 5. $PI(4,5)P_2$ clusters form via electrostatic interactions between positively charged cations and negatively charged phosphate groups.

In the absence of multivalent cations or polybasic proteins, hydrogen bonding networks between $PI(4,5)P_2$ headgroups might induce $PI(4,5)P_2$ clustering despite electrostatic repulsion between highly negatively charged $PI(4,5)P_2$. Support for this hypothesis comes from the fact that demixing of $PI(4,5)P_2$ in fluid phosphatidylcholine (PC) bilayers can occur at membrane concentrations as low as 1% (14). Using Förster resonance energy transfer (FRET), $PI(4,5)P_2$ segregation from PC was observed at high pH, probably stabilized by hydrogen bond networks formed between the hydroxyl groups and the phosphomonoester and phosphodiester groups of adjacent $PI(4,5)P_2$. An NMR study (19) reported that $PI(4,5)P_2$ exhibited a biphasic pH-dependent ionization behavior, which could be explained by intermolecular sharing of the last remaining proton between the vicinal phosphomonoester groups. Strikingly, two studies (15, 18) showed that 5–20 mol% $PI(4,5)P_2$ induced macroscopic phase separation in giant unilamellar vesicles (GUVs) in the presence of 20 mol% PI or cholesterol while using multivalent cation-free buffers. PI was suggested to form a separate phase with $PI(4,5)P_2$, whereas cholesterol was observed to be present in both phases. The presence of such extremely large fractions of $PI(4,5)P_2$ in membranes and the absence of multivalent cations are not physiological conditions, so this kind of macroscopic phase separation might not occur at physiological $PI(4,5)P_2$ levels. It has also been reported that cholesterol, but not cholesterol derivatives with the hydroxyl group modified, promoted and stabilized $PI(4,5)P_2$ domains (15). This result indicates that the cholesterol hydroxyl group might participate in intermolecular hydrogen bond formation. Other bulk lipid components such as phosphatidylethanolamine (PE) could also influence $PI(4,5)P_2$ ionization properties, perhaps serving as hydrogen bond donors (17). A different group showed that the presence of chaotropic agents, such as monovalent salts, urea, and temperature, specifically and significantly expanded the $PI(4,5)P_2$ molecular area in lipid monolayers (135). These results indicate that without multivalent cations, hydrogen bond networks might cluster $PI(4,5)P_2$ and reduce the area per $PI(4,5)P_2$, forming condensed $PI(4,5)P_2$ clusters. Taken together, hydrogen bonding networks might contribute to $PI(4,5)P_2$ cluster formation; however, charge bridging by multivalent cations and charge shielding by proteins seem to play dominant roles under physiological conditions (**Figure 2**).

$PI(4,5)P_2$ binding to multivalent cations has been reported in both monolayers and bilayers. Early investigations found cation binding to $PI(4,5)P_2$ outside the context of membrane bilayers. Ca^{2+} or Mg^{2+} dramatically affected the elution profile of $PI(4,5)P_2$ through an ion exchange column, probably by decreasing the effective charge of $PI(4,5)P_2$ when a stable chelate formed (136). Ca^{2+} or Mg^{2+} binding to $PI(4,5)P_2$ induced large multilamellar $PI(4,5)P_2$ aggregates (137). Later, in both model membranes and red blood cell membranes, cation binding to $PI(4,5)P_2$ revealed that $PI(4,5)P_2$ has higher affinity for Ca^{2+} than for Mg^{2+} (138, 139). Studies of Langmuir monolayers showed that divalent cations bind to $PI(4,5)P_2$ (140). In contrast to chaotropic agents such as monovalent salts, which expanded the area per $PI(4,5)P_2$ molecule in monolayers, Ca^{2+} significantly condensed the area per $PI(4,5)P_2$ molecule. Surface pressure measurements showed that this condensing effect is reversible. The addition of Ca^{2+} decreased the surface pressure in a constant monolayer area. The surface pressure recovered to the normal level upon adding an excess of EDTA to chelate all of the Ca^{2+} (141). Additional studies on membrane bilayers provided more details of $PI(4,5)P_2$ and multivalent cation association. Based on electrophoretic mobility measurements (21), the intrinsic association constants of Ca^{2+} and Mg^{2+} for $PI(4,5)P_2$ were 500 M^{-1} and 100 M^{-1}, respectively. Based on surface potential measurements, another study reported that the calculated intrinsic association constants for $PI(4,5)P_2$ in bilayers were 360 M^{-1} for Ca^{2+} and 220 M^{-1} for Mg^{2+} (141). Attenuated total reflection Fourier transform infrared measurements suggest that upon binding to $PI(4,5)P_2$ headgroups, partial water loss occurs from the hydration shell of Ca^{2+} but not Mg^{2+}, presumably due to the tight binding of Mg^{2+} to water molecules.

Collectively, these studies provide evidence of Ca^{2+} and Mg^{2+} binding tightly to $PI(4,5)P_2$ headgroups and indicate cluster promotion occurs upon binding under physiological ionic conditions.

Several groups have visualized divalent cation–induced $PI(4,5)P_2$ cluster formation on monolayers, bilayers, or cell membranes. When including fluorescently labeled $PI(4,5)P_2$, Ca^{2+}-dependent $PI(4,5)P_2$ clusters were seen in monolayers at $PI(4,5)P_2$ concentrations between 8 and 50 mol% by using fluorescence microscopy (140). Ellenbroek et al. (142) published $PI(4,5)P_2$ phase diagrams in monolayers with 1 mM Ca^{2+} based on atomic force microscopy (AFM) and fluorescence microscopy. They showed that divalent cation–induced $PI(4,5)P_2$ clusters were visible at as low as 2 mol% $PI(4,5)P_2$ at pH 7.4. Using supported lipid monolayers, the same group later used tapping mode AFM imaging to visualize submicrometer-sized $PI(4,5)P_2$ clusters with a radius of approximately 40 nm induced by micromolar Ca^{2+} and smaller clusters induced by millimolar Mg^{2+} (141). A different group found that in the absence of divalent cations, GUVs that contain 5 mol% total $PI(4,5)P_2$ and 0.1% fluorescent $PI(4,5)P_2$ looked uniform. Divalent cations induced $PI(4,5)P_2$ cluster formation in a concentration-dependent manner above 25 μM for Ca^{2+} and above 300 μM for Mg^{2+}. Furthermore, the presence of high concentrations of divalent cations (>300 μM for Ca^{2+} and >1 mM for Mg^{2+}) rendered the GUVs more fragile and caused vesicle rupture (122). However, a different group (143) did not observe $PI(4,5)P_2$ clusters in GUVs containing 1 mol% $PI(4,5)P_2$ with 100 μM Ca^{2+}. Their fluorescence depolarization data implied that an average cluster has approximately 15 $PI(4,5)P_2$ molecules. $PI(4,5)P_2$ clusters on cell membrane sheets have been visualized primarily by $PI(4,5)P_2$-specific binding proteins with fluorescent tags, such as PH-PLCδ, or by $PI(4,5)P_2$ antibodies, via use of fluorescence microscopic methods. For example, one group (119) used dSTORM to image PC12 cell membrane sheets with anti$PI(4,5)P_2$ antibodies directly conjugated with Alexa Fluor 647. They estimated the $PI(4,5)P_2$ cluster size to be ~65 nm. As mentioned in Section 6, Honigmann et al. (123) used STED microscopy to find that $PI(4,5)P_2$ clusters in PC12 cell membranes had an average diameter of ~70 nm when detected with fluorescent PH-PLCδ and an average diameter of ~90 nm when detected by a monoclonal $PI(4,5)P_2$ antibody plus a secondary antibody labeled with Alexa Fluor 488. In summary, these imaging studies on monolayers, GUVs, and cell membrane sheets indicate that $PI(4,5)P_2$–cation clusters are most likely to be submicroscopic by conventional confocal microscopy. The size of these nanoscopic $PI(4,5)P_2$ clusters could be determined only by using superresolution microscopy with optimized labeling methods. It has been possible to create spatial patterns of PI(4)P and $PI(4,5)P_2$ in confined regions of supported lipid bilayers, in the presence of both PIP5K and 5′-phosphatases, when the reaction was geometrically confined (144). Stochastic geometry sensing might provide a mechanism for creating lipid gradients in confined structures, such as membrane sheets, blebs, vesicles, and tubules. These spatial patterns of PI(4)P and $PI(4,5)P_2$ were visualized with fluorescent DrrA (a Rab recruitment protein) and PH-PLCδ, respectively. However, the reaction buffer used in this study contained 5 mM Mg^{2+}, which can induce clustering of both PI(4)P and $PI(4,5)P_2$, even in the absence of enzymes. The influence of fluorescent protein probes like PH-PLCδ or fluorescent lipid antibodies on cluster formation and size should be carefully investigated.

Determining lipid lateral diffusion is crucial for understanding membrane spatial heterogeneity. Another way to confirm $PI(4,5)P_2$ clustering is to determine whether $PI(4,5)P_2$ molecular diffusion slows down in the membrane. Lipid diffusion has been studied in model membranes and intact cell membranes by methods such as fluorescence correlation spectroscopy (FCS) and fluorescence recovery after photobleaching (FRAP) (145). The Prieto group (143) detected Ca^{2+}-induced clustering of $PI(4,5)P_2$ with FCS. The diffusion coefficient of $PI(4,5)P_2$ decreased in the presence of 100 μM Ca^{2+}, while that of the control lipid POPS (palmitoyl

oleoyl phosphatidylserine) remained unchanged. This study concluded that the high sensitivity of $PI(4,5)P_2$ diffusion to Ca^{2+} indicates that $PI(4,5)P_2$ cluster size must be larger than dimers. The Janmey group (141) also used FCS to detect cation-induced slowing of $PI(4,5)P_2$ diffusion in GUVs. The presence of 1 mM Mg^{2+} slowed the diffusion of fluorescently labeled $PI(4,5)P_2$ by fourfold, consistent with nanoscopic $PI(4,5)P_2$ clusters being induced by Mg^{2+}. Compared with Mg^{2+} and Zn^{2+}, Ca^{2+} slowed $PI(4,5)P_2$ diffusion more. The McLaughlin group (73) reported that the diffusion of $PI(4,5)P_2$ is 10 times slower in the presence of micromolar Ca^{2+}. This study also showed that in the presence of 1 mol% $PI(4,5)P_2$ in GUVs, the diffusion rate of a membrane-associated fluorescently labeled polybasic peptide, Lys13, is only approximately half of that in a $PI(4,5)P_2$-free membrane, indicating that the polybasic peptide diffuses together with the laterally sequestered $PI(4,5)P_2$. This result suggests that there can be two different $PI(4,5)P_2$ populations present in the PM. Another paper from this group (146) further explored $PI(4,5)P_2$ diffusion in the PM of fibroblasts and epithelial cells, as well as in model membranes like GUVs. They used fluorescent $PI(4,5)P_2$ to label either the outer leaflet by incubating GUVs with $PI(4,5)P_2$-containing micelles or the inner leaflet by microinjecting $PI(4,5)P_2$-containing micelles into GUVs. They reported that $PI(4,5)P_2$ diffusion at the cellular inner leaflet of the PM was two- to fourfold slower than the $PI(4,5)P_2$ diffusion at the cellular outer leaflet of the PM, in PM-derived blebs, and on GUVs. The lower diffusion coefficient of $PI(4,5)P_2$ in the inner leaflet is consistent with the hypothesis that approximately two thirds of the $PI(4,5)P_2$ is reversibly and electrostatically associated with multivalent cations and basic membrane proteins or the cytoskeleton, while the rest of the $PI(4,5)P_2$ is free. Together, these studies provide strong evidence that the $PI(4,5)P_2$ diffusion rate slows down significantly when $PI(4,5)P_2$ cluster formation occurs as a result of multivalent cation bridging and sequestration by cellular proteins.

Since $PI(4,5)P_2$–cation clusters are most likely to be nanoscopic, biophysical methods such as FRET, fluorescence self-quenching, and fluorescence anisotropy are required to provide molecular details about these clusters. The Janmey group (141) used FRET to study divalent cation–induced $PI(4,5)P_2$ clustering in membrane bilayers and found that the trend in inducing $PI(4,5)P_2$ cluster formation follows the order of $Ca^{2+} \gg Mg^{2+} > Zn^{2+}$ at a fixed 5 mol% $PI(4,5)P_2$. Using fluorescence anisotropy, the Prieto group (143) reported that Ca^{2+} at concentrations up to 100 μM induces $PI(4,5)P_2$ clusters. At identical concentrations, Ca^{2+} is significantly more efficient than Mg^{2+} at promoting $PI(4,5)P_2$ clustering (147), but 5 mM Mg^{2+} was able to drive $PI(4,5)P_2$ clustering more efficiently than 100 μM Ca^{2+}. The Prieto group (143) also used fluorescence self-quenching to investigate the $PI(4,5)P_2$ lateral distribution in PC bilayers. The steady-state fluorescence intensity of TopFluor–$PI(4,5)P_2$ was measured at several concentrations. Self-quenching was observed as Ca^{2+} concentration increased, with no self-quenching seen in the presence of 5 mM EDTA for up to 1 mol% total $PI(4,5)P_2$ (143). Most previous studies focused only on the effect of physiological cations such as Ca^{2+} with the Ca^{2+}-free condition as the negative control. However, without adding the metal chelators EDTA or EGTA to buffers, or without using CHELEX-treated buffers, other multivalent cations are likely to be present (148). Discrepancies in the $PI(4,5)P_2$ literature come from multivalent cation contamination in buffers, as we showed recently (131). Thus, careful sample and buffer preparation is necessary to study $PI(4,5)P_2$ behavior.

Although $PI(4,5)P_2$ clustering is supported by abundant evidence, most previous in vitro studies used nonphysiological $PI(4,5)P_2$ concentrations greater than 5 mol% and buffers containing uncharacterized multivalent cation contamination. Our recent study (131) showed that buffers prepared with American Chemical Society–grade chemicals with 99% purity and stored in borosilicate glass bottles contained Ca^{2+} (60 μM), Al^{3+} (10 μM), Zn^{2+} (6 μM), and Fe^{3+} (0.1 μM) by measurement with inductively coupled plasma optical emission spectroscopy.

Characterizing $PI(4,5)P_2$ behavior at high $PI(4,5)P_2$ concentrations misses the origin of $PI(4,5)P_2$–$PI(4,5)P_2$ association. Recently, we found a maximal solubility of free $PI(4,5)P_2$ in model membranes, above which $PI(4,5)P_2$ clustering occurs in the presence of multivalent cations. Both self-quenching and FRET were used to examine $PI(4,5)P_2$ self-aggregation behavior over a 200-fold concentration range from 0.01 to 2 mol% in model bilayers that mimic the inner leaflet lipid composition, including PE, PS, and cholesterol, in buffers with known cation types and concentrations. $PI(4,5)P_2$ starts to self-associate at extremely low concentrations of 0.02–0.05 mol% of total lipids, with multivalent cations absolutely required for this type of $PI(4,5)P_2$ clustering. The maximal $PI(4,5)P_2$ solubility prior to clustering was termed the critical $PI(4,5)P_2$ concentration (CPC) by analogy with the CMC. This type of $PI(4,5)P_2$ association was described to be $PI(4,5)P_2$–cation clustering because EDTA eliminates the $PI(4,5)P_2$ clusters. For both FRET and self-quenching, the linear increase with increasing $PI(4,5)P_2$ above the CPC implies that all additional $PI(4,5)P_2$ forms more clusters that possess the same properties. This abrupt onset of $PI(4,5)P_2$ self-association is a characteristic of high-order aggregation, as seen in micelle formation or phase separation. $PI(4,5)P_2$–cation cluster formation is not dependent on a particular multivalent cation. Al^{3+} had the strongest effect on cluster formation and Mg^{2+} the weakest, but a variety of cations promoted clustering, including Ca^{2+}, Zn^{2+}, and Fe^{3+}. As low as 1 μM of Al^{3+}, Ca^{2+}, Fe^{3+}, or Zn^{2+} or 50 μM Mg^{2+} was enough to cause $PI(4,5)P_2$ clustering above the CPC in a buffer containing 100 mM KCl and 20 mM HEPES. Many previous studies did not consider the possible multivalent cation contaminants present in the micromolar range in salts and buffers. Moreover, metal ions are leached from glass and plastic over time, complicating the interpretation of some previous reports on $PI(4,5)P_2$ behavior.

We pointed out that $PI(4,5)P_2$ clustering is a headgroup-specific behavior that is not influenced by the $PI(4,5)P_2$ hydrophobic acyl chain types (131). Another important finding is that other PIP species can cocluster with $PI(4,5)P_2$, but PI cannot. This result indicates that the phosphate groups at positions 3, 4, or 5 of the inositol ring are required for the coclustering, with positively charged multivalent cations bridging the negatively charged phosphomonoesters. Thus, pools of different PIPs could exist; for example, PI(4)P and $PI(4,5)P_2$ could coexist within the same cluster at the inner leaflet of the PM. While multivalent cations are absolutely required for $PI(4,5)P_2$–cation cluster formation, the bulk membrane composition surrounding the $PI(4,5)P_2$ also influences $PI(4,5)P_2$ clustering. For example, self-quenching of fluorescent TopFluor–$PI(4,5)P_2$ in PE/PI/cholesterol bilayers is sixfold higher than in PC bilayers. Cholesterol or PI promotes even more clustering, though the mechanism is unclear. Physiological levels of 0.5 mM Mg^{2+} that mimic the resting state in cells are sufficient to induce physiological levels of 2 mol% $PI(4,5)P_2$ to cluster; an additional 100 μM Ca^{2+}, mimicking local transient cellular calcium influx, causes even stronger $PI(4,5)P_2$ clustering. In summary, this study sheds light on how $PI(4,5)P_2$ exists as spatially separated pools in cells, because it quantitatively pinpoints several experimental factors that affect clustering in vitro.

8. HOW PROTEINS RECOGNIZE AND RESPOND TO $PI(4,5)P_2$ CLUSTERS

In the cytosol, the total concentration of $PI(4,5)P_2$-binding proteins far exceeds that of $PI(4,5)P_2$ at the inner leaflet, implying that $PI(4,5)P_2$ clustering could be highly regulated. In this review, we show that four properties of this unique lipid are key to its behavior (**Figure 3**): (*a*) Both free and clustered forms of $PI(4,5)P_2$ can coexist in the same membrane, (*b*) the lateral distribution of $PI(4,5)P_2$ is regulated by a variety of bound molecules, (*c*) different proteins preferentially bind to

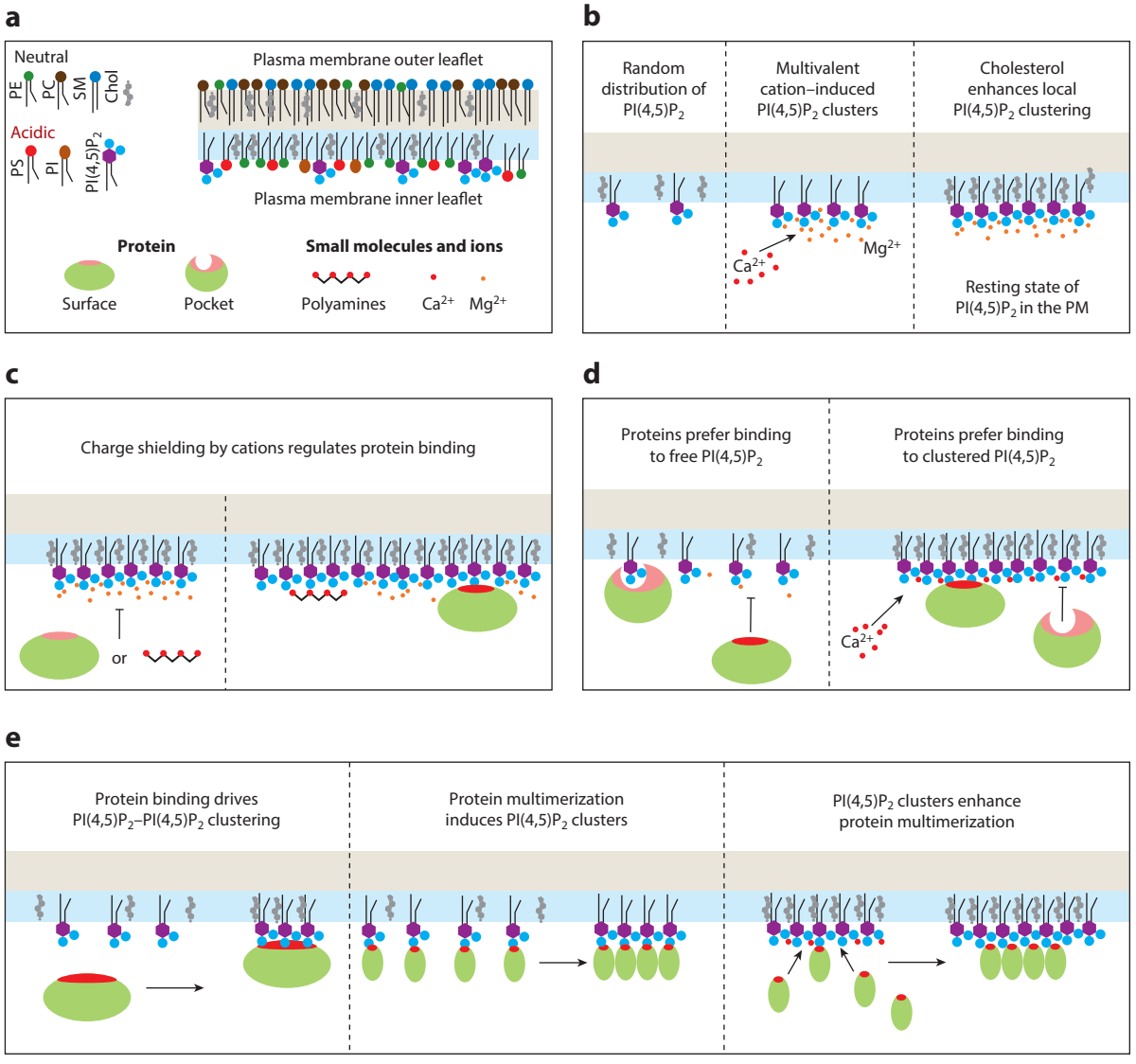

Figure 3

Different modes of protein response to $PI(4,5)P_2$ clusters. (*a*) The asymmetric lipid distribution across the PM. (*b*) $PI(4,5)P_2$ clusters can form in the presence of physiological multivalent cations. Spatially separated pools of free and clustered $PI(4,5)P_2$ coexist at the inner leaflet of the PM. (*c*) Charge shielding and sequestration of negatively charged $PI(4,5)P_2$ headgroups by cations and polybasic small molecules regulate protein binding to $PI(4,5)P_2$. (*d*) Some proteins prefer to bind free $PI(4,5)P_2$, while others bind $PI(4,5)P_2$ in clusters. During transient calcium influx or any local cation changes, proteins targeting to free $PI(4,5)P_2$ could have reduced binding, while proteins targeting to clustered $PI(4,5)P_2$ could have enhanced binding. (*e*) Upon membrane binding, some proteins can sequester local $PI(4,5)P_2$. Some proteins induce $PI(4,5)P_2$ cluster formation as they multimerize on membranes; in turn, multimerized proteins have enhanced membrane binding. Abbreviations: Chol, cholesterol; PC, phosphatidylcholine; PE, phosphatidylethanolamine; PI, phosphatidylinositol; $PI(4,5)P_2$, phosphatidylinositol 4,5-bisphosphate; PM, plasma membrane; PS, phosphatidylserine; SM, sphingomyelin.

free and/or clustered PI(4,5)P_2, and (*d*) multimerization of PI(4,5)P_2-bound proteins can further modulate PI(4,5)P_2 clustering properties.

8.1. Both Free and Clustered Forms of PI(4,5)P_2 Can Coexist in the Same Membrane

Separated pools of free and clustered PI(4,5)P_2 can coexist in the same membrane (**Figure 3*a*,*b***). PI(4,5)P_2–cation clusters form at extremely low concentrations within model membranes, a new behavior of PI(4,5)P_2 that we propose also occurs within cell membranes (131). PI(4,5)P_2 clusters can form by local multivalent cations bridging PI(4,5)P_2 headgroups. In a cellular resting state, there is some free PI(4,5)P_2, but most is clustered PI(4,5)P_2 due to the presence of Mg^{2+} and binding proteins. During transient Ca^{2+} influx, local PI(4,5)P_2 clustering is enhanced. Moreover, PI(4,5)P_2 clustering can be influenced by the local lipid environment; for example, cholesterol seems to enhance local PI(4,5)P_2 clustering. In the presence of PI(4,5)P_2-interacting proteins, protein-induced PI(4,5)P_2 clusters could also form (149). All of these local factors collectively contribute to these spatially separated pools of free, mildly clustered, or tightly clustered PI(4,5)P_2, which could further regulate protein-binding events.

8.2. The Lateral Distribution of PI(4,5)P_2 Is Regulated by a Variety of Bound Molecules

PI(4,5)P_2 cluster–inducing binders such as multivalent cations, polyamines, and proteins with basic patches regulate PI(4,5)P_2 properties and further regulate other cellular factors having access to PI(4,5)P_2 (**Figure 3*c***). Although the PI(4,5)P_2 concentration in the PM cytosolic leaflet is 1–2 mol%, a majority of this PI(4,5)P_2 must be sequestered by proteins or by multivalent cations. The lateral organization and function of PI(4,5)P_2 could undergo significant changes in the presence of physiologically relevant concentrations of multivalent cations, which influence PI(4,5)P_2-dependent cellular processes. One study (150) found that intracellular Mg^{2+} inhibits a PI(4,5)P_2-requiring ion channel called KCNQ2/3. Mg^{2+} reduced the current by electrostatically binding to PI(4,5)P_2, significantly reducing the free PI(4,5)P_2 available for interaction with these channels. This mechanism is likely to modulate many other PI(4,5)P_2-dependent ion channels and cellular processes. In another example, Mg^{2+} and polyamines electrostatically bind to PI(4,5)P_2 and could inhibit the activity of PLC by decreasing the amount of free PI(4,5)P_2 available for hydrolysis (151). The homeostasis of metal cations is modulated by different transporters (152). The transient influx upon signaling activation by metal ions such as Ca^{2+} or Zn^{2+} could potentially regulate PI(4,5)P_2 lateral distribution in the membrane and accessibility to other PI(4,5)P_2-binding proteins. The details of electrostatic charge shielding of PI(4,5)P_2 by multivalent cations, polyamines, and polybasic proteins would differ based on the membrane charge density, ionic radius, dehydration energy of cations, and manner of bringing together multiple charges. However, one final result could be similar: Shielding and sequestering negatively charged PI(4,5)P_2 headgroups prevent PI(4,5)P_2 from interacting with certain binding molecules (**Figure 3*c***).

8.3. Different Proteins Preferentially Bind to Free and/or Clustered PI(4,5)P_2

Some proteins prefer to bind free PI(4,5)P_2 while others prefer to bind PI(4,5)P_2 in clusters (**Figure 3*d***). Several, or even many, populations of PI(4,5)P_2 could coexist depending on local multivalent cation concentration and local lipid concentration, and free PI(4,5)P_2 could be in equilibrium with clustered PI(4,5)P_2. The headgroup of free PI(4,5)P_2 is exposed, and thus

proteins that preferentially bind to sparsely distributed free $PI(4,5)P_2$ would have immediate access. The headgroup of clustered $PI(4,5)P_2$ must be bound by cations or proteins; those proteins that preferentially bind to clustered $PI(4,5)P_2$ would be competing against bound cations for access to $PI(4,5)P_2$ molecules. $PI(4,5)P_2$–cation clusters could form a two-dimensional array of the many $PI(4,5)P_2$ phosphate groups together with multivalent cations. The degree of $PI(4,5)P_2$–cation clustering would depend on the type and concentration of multivalent cations and on the surrounding lipid compositions. Local changes to multivalent cations and surrounding lipids affect the free and clustered $PI(4,5)P_2$ concentrations, thus further influencing $PI(4,5)P_2$-binding protein types, concentrations, and functions. For example, during a transient calcium influx, more cation-bridged $PI(4,5)P_2$ clusters would form, and the proteins that target clustered $PI(4,5)P_2$ could experience enhanced function, while proteins that target free $PI(4,5)P_2$ could experience decreased function (**Figure 3*d***). Our recent study shows that a fluorescent version of PH-PLCδ1 exhibits robust binding to free $PI(4,5)P_2$ on GUVs but reduced binding to clustered $PI(4,5)P_2$ bridged by multivalent cations (149). The stronger the degree of $PI(4,5)P_2$ clustering on GUVs, the less overall membrane binding of PH-PLCδ1.

Several reasons might explain why proteins bind preferentially to free $PI(4,5)P_2$ on the one hand or to clustered $PI(4,5)P_2$ on the other. PH-PLCδ1 and similar proteins contain a canonical $PI(4,5)P_2$ binding pocket that is proposed to interact with the $PI(4,5)P_2$ headgroup with 1:1 stoichiometry in a noncooperative manner (57). Multivalent cations binding to $PI(4,5)P_2$ headgroups are reported to confine the lipid headgroup tilt angle, which based on molecular dynamics simulations would inhibit PH-PLCδ1-domain recognition (153). Unlike PH-PLCδ1 with its canonical $PI(4,5)P_2$-binding site, proteins with a polybasic region or patch, such as MARCKS and N-WASP, bind to $PI(4,5)P_2$ in a multivalent manner. The activation of N-WASP has been shown to depend on $PI(4,5)P_2$ concentration; once the $PI(4,5)P_2$ level is above a threshold, N-WASP binds to $PI(4,5)P_2$ cooperatively with an apparent Hill coefficient of approximately 20. This sharp $PI(4,5)P_2$ sensitivity can be tuned by modulating the polybasic region (154). We recently reported that naturally myristoylated HIV-1 MA preferentially binds to clustered $PI(4,5)P_2$ over free $PI(4,5)P_2$, while the nonmyristoylated mutant strongly binds to free $PI(4,5)P_2$ (149). The naturally nonmyristoylated RSV MA also preferentially binds to free $PI(4,5)P_2$. However, the forced hexameric version of RSV MA exhibits the opposite binding profile, preferring binding to clustered $PI(4,5)P_2$ over free $PI(4,5)P_2$. From these results we propose that only proteins with strong membrane affinity can compete with $PI(4,5)P_2$-shielding multivalent cations to gain access to $PI(4,5)P_2$ headgroups, while proteins with weak membrane affinity have access to free $PI(4,5)P_2$ headgroups but not to headgroup-shielded $PI(4,5)P_2$.

8.4. Multimerization of $PI(4,5)P_2$-Bound Proteins Can Further Modulate $PI(4,5)P_2$ Clustering Properties

Clustering of $PI(4,5)P_2$-bound proteins could sequester $PI(4,5)P_2$ or even induce $PI(4,5)P_2$ clustering (**Figure 3*e***), especially if those proteins can multimerize on membranes. Clustered $PI(4,5)P_2$ could then recruit more proteins to achieve downstream functions. The behavior of syntaxin-1 in PC12 cells (120) shows that clustering of membrane-bound proteins can lead to formation of $PI(4,5)P_2$ clusters by electrostatic interactions with juxtamembrane basic residues. Another example of protein multimerization leading to $PI(4,5)P_2$ clusters involves the BAR superfamily of proteins. The I-BAR, F-BAR, and N-BAR domains from many mammalian proteins have been shown to induce $PI(4,5)P_2$ clustering (155, 156). These BAR domains assemble into stable scaffolds to bend membranes and restrict $PI(4,5)P_2$ lateral diffusion by generating stable $PI(4,5)P_2$–BAR domain clusters. Besides $PI(4,5)P_2$, BAR domains could also cluster $PI(3,4,5)P_3$

and phosphatidylinositol 3-phosphate (PI3P), indicating that this clustering occurs through electrostatic sequestration. Several studies show that the PH domain of dynamin-1 and -2 binds to $PI(4,5)P_2$ with low affinity and a K_d value above 1 mM (157). However, oligomerization of dynamin can locally cluster $PI(4,5)P_2$ at coated pits. Concentrated $PI(4,5)P_2$ allows multiple PH domains to interact with membranes with higher affinity, promoting vesicle scission during CME (158, 159).

Similar to clustering by cellular proteins, $PI(4,5)P_2$ sequestration can be induced by viral proteins. $PI(4,5)P_2$ enrichment in HIV-1 viral membranes and the efficient self-assembly of the Gag protein have led to competing, but not mutually exclusive, hypotheses: First, $PI(4,5)P_2$-rich domains preexist and are targeted by Gag; second, $PI(4,5)P_2$ clustering is induced by Gag multimerization during assembly (160, 161). Our recent study provides comprehensive evidence that Gag assembly on membranes induces $PI(4,5)P_2$ clusters (149). Both specific $PI(4,5)P_2$ interactions and Gag–Gag interactions are required for this protein-induced $PI(4,5)P_2$ clustering effect, as the relevant mutants fail to cluster $PI(4,5)P_2$. Protein-induced $PI(4,5)P_2$ clustering and multivalent cation–induced $PI(4,5)P_2$ clustering are independent and additive. Collectively, we show that HIV-1 Gag not only targets preexisting $PI(4,5)P_2$ clusters but also further enriches $PI(4,5)P_2$ at assembly sites while Gag multimerizes. $PI(4,5)P_2$ clustering and protein multimerization are likely to facilitate each other, creating membrane platforms for optimal protein function.

9. CONCLUSIONS AND OUTSTANDING QUESTIONS

The rich physical chemistry of $PI(4,5)P_2$ contributes to its being an interesting and important phospholipid in cells. Despite electrostatic repulsion, $PI(4,5)P_2$ can form clusters via two major attractive interactions—hydrogen bonding and, especially, multivalent cation bridging, with the latter likely having the predominant role in cells. Spatially separated pools of $PI(4,5)P_2$ could arise from localized $PI(4,5)P_2$ aggregation due to local differences in multivalent cations and lipid compositions as well as to localized $PI(4,5)P_2$ synthesis and breakdown. $PI(4,5)P_2$ clustering changes the orientation and accessibility of the headgroups, and this has many implications for the biological function of this phospholipid. A given protein is likely to preferentially bind to either free $PI(4,5)P_2$ or clustered $PI(4,5)P_2$; $PI(4,5)P_2$-bound proteins are also likely to either promote or disrupt preexisting $PI(4,5)P_2$ clusters. Tight control of local synthesis and turnover of $PI(4,5)P_2$, together with well-regulated cluster formation and recruitment of selected proteins to specific sites at the inner leaflet of the PM, create a broad spectrum of $PI(4,5)P_2$-dependent cellular functions.

$PI(4,5)P_2$ clusters likely exist in all cells and are recognized and utilized by hundreds of cellular proteins, so understanding the nature of $PI(4,5)P_2$ behavior is fundamental to cell biology. It is of great importance to further investigate the biophysical properties of $PI(4,5)P_2$–cation and $PI(4,5)P_2$–protein clusters, especially upon cellular protein binding, transient calcium influx, or zinc sparks. The last is a fertilization event that induces the exocytotic release of billions of zinc ions (162). Only when we have a better understanding of this unique lipid will we be able to seek answers for more complicated questions. In the future, it is critical to elucidate the mechanisms by which $PI(4,5)P_2$, an inner leaflet lipid, is mysteriously found associated with rafts in PM outer leaflet microdomains. Many enveloped viruses other than HIV-1 likely also rely on $PI(4,5)P_2$ clusters to assemble progeny viral particles and then bud from infected cells; perhaps this specific $PI(4,5)P_2$ dependence could be these viruses' Achilles' heel.

SUMMARY POINTS

1. Diverse cellular and viral proteins interact with $PI(4,5)P_2$ using different binding strategies, such as surface electrostatic interactions or a specific binding pocket.
2. $PI(4,5)P_2$ starts to self-associate at extremely low concentrations in membrane bilayers, forming nanoscopic $PI(4,5)P_2$ clusters with headgroups bridged by multivalent cations.
3. Other PIP species are able to cocluster with $PI(4,5)P_2$ due to positively charged multivalent cations bridging the negatively charged phosphomonoesters.
4. Differences in local multivalent cation types and concentrations, as well as the surrounding lipid environments, could significantly influence local $PI(4,5)P_2$ clustering, resulting in spatially separated pools of free and clustered $PI(4,5)P_2$.
5. Electrostatic shielding and sequestration of $PI(4,5)P_2$ headgroups by multivalent cations and proteins with basic patches regulate $PI(4,5)P_2$ accessibility to other $PI(4,5)P_2$ binders.
6. Some cellular and viral proteins preferentially bind to free $PI(4,5)P_2$, some preferentially bind to clustered $PI(4,5)P_2$, and others do not have a preference.
7. Proteins binding to $PI(4,5)P_2$, especially those that can multimerize, can laterally sequester $PI(4,5)P_2$ or induce $PI(4,5)P_2$ clustering electrostatically.

DISCLOSURE STATEMENT

The authors are not aware of any affiliations, memberships, funding, or financial holdings that might be perceived as affecting the objectivity of this review.

ACKNOWLEDGMENTS

We thank Robert A. Dick for figure preparation, discussions, and editing. This work was supported by the National Institutes of Health (awards R01-AI150454 to V.M.V., R01-GM1045684 to G.W.F., and R01-AI147890 to Robert A. Dick).

LITERATURE CITED

1. Hokin M, Hokin L. 1953. Enzyme secretion and the incorporation of P^{32} into phospholipides of pancreas slices. *J. Biol. Chem.* 203(2):967–77
2. Wiedemann C, Cockcroft S. 1998. The role of phosphatidylinositol transfer proteins (PITPs) in intracellular signalling. *Trends Endocrinol. Metab.* 9(8):324–28
3. Phillips SE, Vincent P, Rizzieri KE, Schaaf G, Bankaitis VA, Gaucher EA. 2006. The diverse biological functions of phosphatidylinositol transfer proteins in eukaryotes. *Crit. Rev. Biochem. Mol. Biol.* 41(1):21–49
4. Lipp NF, Ikhlef S, Milanini J, Drin G. 2020. Lipid exchangers: cellular functions and mechanistic links with phosphoinositide metabolism. *Front. Cell Dev. Biol.* 8:663
5. Shewan A, Eastburn DJ, Mostov K. 2011. Phosphoinositides in cell architecture. *Cold Spring Harb. Perspect. Biol.* 3(8):a004796
6. Di Paolo G, De Camilli P. 2006. Phosphoinositides in cell regulation and membrane dynamics. *Nature* 443(7112):651–57
7. Toker A. 1998. The synthesis and cellular roles of phosphatidylinositol 4,5-bisphosphate. *Curr. Opin. Cell Biol.* 10(2):254–61

8. Martin TF. 2001. PI(4,5)P_2 regulation of surface membrane traffic. *Curr. Opin. Cell Biol.* 13(4):493–99
9. Balla T. 2013. Phosphoinositides: tiny lipids with giant impact on cell regulation. *Physiol. Rev.* 93(3):1019–137
10. McLaughlin S, Wang J, Gambhir A, Murray D. 2002. PIP_2 and proteins: interactions, organization, and information flow. *Annu. Rev. Biophys. Biomol. Struct.* 31:151–75
11. Tan X, Thapa N, Choi S, Anderson RA. 2015. Emerging roles of PtdIns(4,5)P_2—beyond the plasma membrane. *J. Cell Sci.* 128(22):4047–56
12. Brown DA. 2015. PIP2 clustering: from model membranes to cells. *Chem. Phys. Lipids* 192:33–40
13. Kwiatkowska K. 2010. One lipid, multiple functions: how various pools of PI(4,5)P_2 are created in the plasma membrane. *Cell. Mol. Life Sci.* 67(23):3927–46
14. Redfern DA, Gericke A. 2004. Domain formation in phosphatidylinositol monophosphate/phosphatidylcholine mixed vesicles. *Biophys. J.* 86(5):2980–92
15. Jiang Z, Redfern RE, Isler Y, Ross AH, Gericke A. 2014. Cholesterol stabilizes fluid phosphoinositide domains. *Chem. Phys. Lipids* 182:52–61
16. Kooijman EE, Gericke A. 2014. Physical chemistry and biophysics of polyphosphoinositide mediated lipid signaling. *Chem. Phys. Lipids* 182:1–2
17. Graber ZT, Gericke A, Kooijman EE. 2014. Phosphatidylinositol-4,5-bisphosphate ionization in the presence of cholesterol, calcium or magnesium ions. *Chem. Phys. Lipids* 182:62–72
18. Graber ZT, Jiang Z, Gericke A, Kooijman EE. 2012. Phosphatidylinositol-4,5-bisphosphate ionization and domain formation in the presence of lipids with hydrogen bond donor capabilities. *Chem. Phys. Lipids* 165(6):696–704
19. Kooijman EE, King KE, Gangoda M, Gericke A. 2009. Ionization properties of phosphatidylinositol polyphosphates in mixed model membranes. *Biochemistry* 48(40):9360–71
20. van Paridon PA, de Kruijff B, Ouwerkerk R, Wirtz KWA. 1986. Polyphosphoinositides undergo charge neutralization in the physiological pH range: a ^{31}P-NMR study. *Biochim. Biophys. Acta Lipids Lipid Metab.* 877(1):216–19
21. Toner M, Vaio G, McLaughlin A, McLaughlin S. 1988. Adsorption of cations to phosphatidylinositol 4,5-bisphosphate. *Biochemistry* 27(19):7435–43
22. Moncelli MR, Becucci L, Guidelli R. 1994. The intrinsic pK_a values for phosphatidylcholine, phosphatidylethanolamine, and phosphatidylserine in monolayers deposited on mercury electrodes. *Biophys. J.* 66(6):1969–80
23. Tsui FC, Ojcius DM, Hubbell WL. 1986. The intrinsic pK_a values for phosphatidylserine and phosphatidylethanolamine in phosphatidylcholine host bilayers. *Biophys. J.* 49(2):459–68
24. Pérez-Lara Á, Thapa A, Nyenhuis SB, Nyenhuis DA, Halder P, et al. 2016. PtdInsP_2 and PtdSer cooperate to trap synaptotagmin-1 to the plasma membrane in the presence of calcium. *eLife* 5:e15886
25. Traynor-Kaplan A, Kruse M, Dickson EJ, Dai G, Vivas O, et al. 2017. Fatty-acyl chain profiles of cellular phosphoinositides. *Biochim. Biophys. Acta Mol. Cell Biol. Lipids* 1862(5):513–22
26. Tong J, Nguyen L, Vidal A, Simon SA, Skene JHP, McIntosh TJ. 2008. Role of GAP-43 in sequestering phosphatidylinositol 4,5-bisphosphate to raft bilayers. *Biophys. J.* 94(1):125–33
27. Simons K, Sampaio JL. 2011. Membrane organization and lipid rafts. *Cold Spring Harb. Perspect. Biol.* 3(10):a004697
28. Pike LJ, Miller JM. 1998. Cholesterol depletion delocalizes phosphatidylinositol bisphosphate and inhibits hormone-stimulated phosphatidylinositol turnover. *J. Biol. Chem.* 273(35):22298–304
29. Hammond GR V. 2016. Does PtdIns(4,5)P_2 concentrate so it can multi-task? *Biochem. Soc. Trans.* 44(1):228–33
30. Johnson CM, Chichili GR, Rodgers W. 2008. Compartmentalization of phosphatidylinositol 4,5-bisphosphate signaling evidenced using targeted phosphatases. *J. Biol. Chem.* 283(44):29920–28
31. Sezgin E, Levental I, Mayor S, Eggeling C. 2017. The mystery of membrane organization: composition, regulation and roles of lipid rafts. *Nat. Rev. Mol. Cell Biol.* 18(6):361–74
32. Falkenburger BH, Jensen JB, Dickson EJ, Suh BC, Hille B. 2010. Phosphoinositides: lipid regulators of membrane proteins. *J. Physiol.* 588(17):3179–85
33. Sun Y, Thapa N, Hedman AC, Anderson RA. 2013. Phosphatidylinositol 4,5-bisphosphate: targeted production and signaling. *BioEssays* 35(6):513–22

34. Hinchliffe K. 2000. Intracellular signalling: Is PIP_2 a messenger too? *Curr. Biol.* 10(3):104–5
35. Berridge MJ, Irvine RF. 1984. Inositol triphosphate, a novel second messenger in cellular transduction. *Nature* 312:315–21
36. Chang CL, Chen YJ, Liou J. 2017. ER-plasma membrane junctions: Why and how do we study them? *Biochim. Biophys. Acta Mol. Cell Res.* 1864(9):1494–506
37. Czech MP. 2000. PIP2 and PIP3: complex roles at the cell surface. *Cell* 100(6):603–6
38. Bunce MW, Bergendahl K, Anderson RA. 2006. Nuclear $PI(4,5)P_2$: a new place for an old signal. *Biochim. Biophys. Acta Mol. Cell Biol. Lipids* 1761(5–6):560–69
39. Koch M, Holt M. 2012. Coupling exo- and endocytosis: an essential role for PIP_2 at the synapse. *Biochim. Biophys. Acta Mol. Cell Biol. Lipids* 1821(8):1114–32
40. Hilgemann DW, Feng S, Nasuhoglu C. 2003. The complex and intriguing lives of PIP_2 with ion channels and transporters. *Sci. Signal.* 2001(111):re19
41. Robertson B. 2007. Regulation of ion channels and transporters by phosphatidylinositol 4,5-bisphosphate. *J. Physiol.* 582(3):901–2
42. Yin HL, Janmey PA. 2003. Phosphoinositide regulation of the actin cytoskeleton. *Annu. Rev. Physiol.* 65:761–89
43. Simonsen A, Wurmser AE, Emr SD, Stenmark H. 2001. The role of phosphoinositides in membrane transport. *Curr. Opin. Cell Biol.* 13(4):485–92
44. Cullen PJ, Cozier GE, Banting G, Mellor H. 2001. Modular phosphoinositide-binding domains—their role in signalling and membrane trafficking. *Curr. Biol.* 11(21):882–93
45. Martin TFJ. 2012. Role of $PI(4,5)P_2$ in vesicle exocytosis and membrane fusion. In *Phosphoinositides II: The Diverse Biological Functions*, ed. T Balla, M Wymann, JD York, pp. 111–30. Subcell. Biochem. 59. Dordrecht, Neth.: Springer
46. Krahn MP, Wodarz A. 2012. Phosphoinositide lipids and cell polarity: linking the plasma membrane to the cytocortex. *Essays Biochem.* 53:15–27
47. Scott CC, Dobson W, Botelho RJ, Coady-Osberg N, Chavrier P, et al. 2005. Phosphatidylinositol-4,5-*bis*phosphate hydrolysis directs actin remodeling during phagocytosis. *J. Cell Biol.* 169(1):139–49
48. Ling K, Schill NJ, Wagoner MP, Sun Y, Anderson RA. 2006. Movin' on up: the role of $PtdIns(4,5)P_2$ in cell migration. *Trends Cell Biol.* 16(6):276–84
49. Skwarek LC, Boulianne GL. 2009. Great expectations for PIP: phosphoinositides as regulators of signaling during development and disease. *Dev. Cell* 16(1):12–20
50. Liu Y, Bankaitis VA. 2010. Phosphoinositide phosphatases in cell biology and disease. *Prog. Lipid Res.* 49(3):201–17
51. Catimel B, Schieber C, Condron M, Patsiouras H, Connolly L, et al. 2008. The $PI(3,5)P_2$ and $PI(4,5)P_2$ interactomes. *J. Proteome Res.* 7(12):5295–313
52. Jost M, Simpson F, Kavran JM, Lemmon MA, Schmid SL. 1998. Phosphatidylinositol-4,5-bisphosphate is required for endocytic coated vesicle formation. *Curr. Biol.* 8(25):1399–404
53. Takenawa T. 2010. Phosphoinositide-binding interface proteins involved in shaping cell membranes. *Proc. Jpn. Acad. Ser. B* 86(5):509–23
54. Saarikangas J, Zhao H, Lappalainen P. 2010. Regulation of the actin cytoskeleton-plasma membrane interplay by phosphoinositides. *Physiol. Rev.* 90(1):259–89
55. Rebecchi MJ, Scarlata S. 1998. Pleckstrin homology domains: a common fold with diverse functions. *Annu. Rev. Biophys. Biomol. Struct.* 27:503–28
56. Lemmon MA. 2008. Membrane recognition by phospholipid-binding domains. *Nat. Rev. Mol. Cell Biol.* 9(2):99–111
57. Ferguson KM, Lemmon MA, Schlessinger J, Sigler PB. 1995. Structure of the high affinity complex of inositol trisphosphate with a phospholipase C pleckstrin homology domain. *Cell* 83(6):1037–46
58. Harlan JE, Hajduk PJ, Yoon HS, Fesik SW. 1994. Pleckstrin homology domains bind to phosphatidylinositol-4,5-bisphosphate. *Nature* 371(16493):168–70
59. Hyvönen M, Macias MJ, Nilges M, Oschkinat H, Saraste M, Wilmanns M. 1995. Structure of the binding site for inositol phosphates in a PH domain. *EMBO J.* 14(19):4676–85
60. Jian X, Tang W-K, Zhai P, Roy NS, Luo R, et al. 2015. Molecular basis for cooperative binding of anionic phospholipids to the PH domain of the Arf GAP ASAP1. *Structure* 23(11):1977–88

61. Vonkova I, Saliba AE, Deghou S, Anand K, Ceschia S, et al. 2015. Lipid cooperativity as a general membrane-recruitment principle for PH domains. *Cell Rep.* 12(9):1519–30
62. Stauffer TP, Ahn S, Meyer T. 1998. Receptor-induced transient reduction in plasma membrane PtdIns(4,5)P_2 concentration monitored in living cells. *Curr. Biol.* 8(6):343–46
63. Várnai P, Balla T. 1998. Visualization of phosphoinositides that bind pleckstrin homology domains: calcium- and agonist-induced dynamic changes and relationship to myo-[^{3}H] inositol-labeled phosphoinositide pools. *J. Cell Biol.* 143(2):501–10
64. Garcia P, Gupta R, Shah S, Morris AJ, Rudge SA, et al. 1995. The pleckstrin homology domain of phospholipase C-δ1 binds with high affinity to phosphatidylinositol 4,5-bisphosphate in bilayer membranes. *Biochemistry* 34(49):16228–34
65. Lemmon MA, Ferguson KM, O'Brien R, Sigler PB, Schlessinger J. 1995. Specific and high-affinity binding of inositol phosphates to an isolated pleckstrin homology domain. *PNAS* 92(23):10472–76
66. Niggli V, Andréoli C, Roy C, Mangeat P. 1995. Identification of a phosphatidylinositol-4,5-bisphosphate-binding domain in the N-terminal region of ezrin. *FEBS Lett.* 376(3):172–76
67. Frame MC, Patel H, Serrels B, Lietha D, Eck MJ. 2010. The FERM domain: organizing the structure and function of FAK. *Nat. Rev. Mol. Cell Biol.* 11(11):802–14
68. Fehon RG, McClatchey AI, Bretscher A. 2010. Organizing the cell cortex: the role of ERM proteins. *Nat. Rev. Mol. Cell Biol.* 11(4):276–87
69. Hamada K, Shimizu T, Matsui T, Tsukita S, Tsukita S, Hakoshima T. 2000. Structural basis of the membrane-targeting and unmasking mechanisms of the radixin FERM domain. *EMBO J.* 19(17):4449–62
70. Legendre-Guillemin V, Wasiak S, Hussain NK, Angers A, McPherson PS. 2004. ENTH/ANTH proteins and clathrin-mediated membrane budding. *J. Cell Sci.* 117(1):9–18
71. Itoh T, Koshiba S, Kigawa T, Kikuchi A, Yokoyama S, Takenawa T. 2001. Role of the ENTH domain in phosphatidylinositol-4,5-bisphosphate binding and endocytosis. *Science* 291(5506):1047–51
72. Arbuzova A, Murray D, McLaughlin S. 1998. MARCKS, membranes, and calmodulin: kinetics of their interaction. *Biochim. Biophys. Acta Rev. Biomembr.* 1376(3):369–79
73. Golebiewska U, Gambhir A, Hangyás-Mihályné G, Zaitseva I, Rädler J, McLaughlin S. 2006. Membrane-bound basic peptides sequester multivalent (PIP_2), but not monovalent (PS), acidic lipids. *Biophys. J.* 91(2):588–99
74. Wang J, Gambhir A, Hangyás-Mihályné G, Murray D, Golebiewska U, McLaughlin S. 2002. Lateral sequestration of phosphatidylinositol 4,5-bisphosphate by the basic effector domain of myristoylated alanine-rich C kinase substrate is due to nonspecific electrostatic interactions. *J. Biol. Chem.* 277(37):34401–12
75. Gambhir A, Hangyás-Mihályné G, Zaitseva I, Cafiso DS, Wang J, et al. 2004. Electrostatic sequestration of PIP_2 on phospholipid membranes by basic/aromatic regions of proteins. *Biophys. J.* 86(4):2188–207
76. Rauch ME, Ferguson CG, Prestwich GD, Cafiso DS. 2002. Myristoylated alanine-rich C kinase substrate (MARCKS) sequesters spin-labeled phosphatidylinositol 4,5-bisphosphate in lipid bilayers. *J. Biol. Chem.* 277(16):14068–76
77. Laux T, Fukami K, Thelen M, Golub T, Frey D, Caroni P. 2000. GAP43, MARCKS, and CAP23 modulate PI(4,5)P_2 at plasmalemmal rafts, and regulate cell cortex actin dynamics through a common mechanism. *J. Cell Biol.* 149(7):1455–72
78. Arni S, Keilbaugh SA, Ostermeyer AG, Brown DA. 1998. Association of GAP-43 with detergent-resistant membranes requires two palmitoylated cysteine residues. *J. Biol. Chem.* 273(43):28478–85
79. Cossart P, Helenius A. 2014. Endocytosis of viruses and bacteria. *Cold Spring Harb. Perspect. Biol.* 6(8):a016972
80. DeTulleo L, Kirchhausen T. 1998. The clathrin endocytic pathway in viral infection. *EMBO J.* 17(16):4585–93
81. Vázquez-Calvo Á, Sobrino F, Martín-Acebes MA. 2012. Plasma membrane phosphatidylinositol 4,5 bisphosphate is required for internalization of foot-and-mouth disease virus and vesicular stomatitis virus. *PLOS ONE* 7(9):e45172

82. Barrero-Villar M, Barroso-Gonzalez J, Cabrero JR, Gordon-Alonso M, Alvarez-Losada S, et al. 2008. PI4P5-kinase Iα is required for efficient HIV-1 entry and infection of T cells. *J. Immunol.* 181(10):6882–88
83. Egger D, Wölk B, Gosert R, Bianchi L, Blum HE, et al. 2002. Expression of hepatitis C virus proteins induces distinct membrane alterations including a candidate viral replication complex. *J. Virol.* 76(12):5974–84
84. Sklan EH, Staschke K, Oakes TM, Elazar M, Winters M, et al. 2007. A Rab-GAP TBC domain protein binds hepatitis C virus NS5A and mediates viral replication. *J. Virol.* 81(20):11096–105
85. Waheed AA, Freed EO. 2018. The role of lipids in retroviral replication. In *Retrovirus-Cell Interactions*, ed. L Parent, pp. 353–99. Cambridge, MA: Acad. Press
86. Ono A, Ablan SD, Lockett SJ, Nagashima K, Freed EO. 2004. Phosphatidylinositol (4,5) bisphosphate regulates HIV-1 Gag targeting to the plasma membrane. *PNAS* 101(41):14889–94
87. Chukkapalli V, Hogue IB, Boyko V, Hu W-S, Ono A, et al. 2008. Interaction between the human immunodeficiency virus type 1 Gag matrix domain and phosphatidylinositol-(4,5)-bisphosphate is essential for efficient Gag membrane binding. *J. Virol.* 82(5):2405–17
88. Mücksch F, Laketa V, Müller B, Schultz C, Kräusslich HG. 2017. Synchronized HIV assembly by tunable PIP_2 changes reveals PIP_2 requirement for stable Gag anchoring. *eLife* 6:e25287
89. Dick RA, Goh SL, Feigenson GW, Vogt VM. 2012. HIV-1 Gag protein can sense the cholesterol and acyl chain environment in model membranes. *PNAS* 109(46):18761–66
90. Olety B, Ono A. 2014. Roles played by acidic lipids in HIV-1 Gag membrane binding. *Virus Res.* 193:108–15
91. Saad JS, Miller J, Tai J, Kim A, Ghanam RH, Summers MF. 2006. Structural basis for targeting HIV-1 Gag proteins to the plasma membrane for virus assembly. *PNAS* 103(30):11364–69
92. Chan R, Uchil PD, Jin J, Shui G, Ott DE, et al. 2008. Retroviruses human immunodeficiency virus and murine leukemia virus are enriched in phosphoinositides. *J. Virol.* 82(22):11228–38
93. Mücksch F, Citir M, Lüchtenborg C, Glass B, Traynor-Kaplan A, et al. 2019. Quantification of phosphoinositides reveals strong enrichment of PIP_2 in HIV-1 compared to producer cell membranes. *Sci. Rep.* 9(1):17661
94. Brügger B, Glass B, Haberkant P, Leibrecht I, Wieland FT, Kräusslich HG. 2006. The HIV lipidome: a raft with an unusual composition. *PNAS* 103(8):2641–46
95. Lorizate M, Sachsenheimer T, Glass B, Habermann A, Gerl MJ, et al. 2013. Comparative lipidomics analysis of HIV-1 particles and their producer cell membrane in different cell lines. *Cell Microbiol.* 15(2):292–304
96. Hamard-Peron E, Juillard F, Saad JS, Roy C, Roingeard P, et al. 2010. Targeting of murine leukemia virus Gag to the plasma membrane is mediated by $PI(4,5)P_2$/PS and a polybasic region in the matrix. *J. Virol.* 84(1):503–15
97. Prchal J, Kroupa T, Ruml T, Hrabal R. 2014. Interaction of Mason-Pfizer monkey virus matrix protein with plasma membrane. *Front. Microbiol.* 4:423
98. Fernandes F, Chen K, Ehrlich LS, Jin J, Chen MH, et al. 2011. Phosphoinositides direct equine infectious anemia virus Gag trafficking and release. *Traffic* 12(4):438–51
99. Inlora J, Chukkapalli V, Derse D, Ono A. 2011. Gag localization and virus-like particle release mediated by the matrix domain of human T-lymphotropic virus type-1 Gag are less dependent on phosphatidylinositol-(4,5)-bisphosphate than those mediated by the matrix domain of HIV-1 Gag. *J. Virol.* 85(8):3802–10
100. Chan J, Dick RA, Vogt VM. 2011. Rous sarcoma virus Gag has no specific requirement for phosphatidylinositol-(4,5)-bisphosphate for plasma membrane association in vivo or for liposome interaction in vitro. *J. Virol.* 85(20):10851–60
101. Johnson KA, Taghon GJF, Scott JL, Stahelin RV. 2016. The Ebola virus matrix protein, VP40, requires phosphatidylinositol 4,5-bisphosphate ($PI(4,5)P_2$) for extensive oligomerization at the plasma membrane and viral egress. *Sci. Rep.* 6:19125
102. Wijesinghe KJ, Stahelin RV. 2016. Investigation of the lipid binding properties of the Marburg virus matrix protein VP40. *J. Virol.* 90(6):3074–85

103. Wallace J, Mlodzianoski MJ, Maginnis MS, Lilieholm J, Mehmood K, et al. 2019. Influenza hemagglutinin modulates phosphatidylinositol (4,5)-bisphosphate membrane clustering. *Biophys. J.* 116(5):893–909
104. Alvarez RA, Barría MI, Chen BK. 2014. Unique features of HIV-1 spread through T cell virological synapses. *PLOS Pathog.* 10(12):e1004513
105. Clapham PR, Weiss RA. 1997. Spoilt for choice of co-receptors. *Nature* 388(6639):230–31
106. Jolly C, Kashefi K, Hollinshead M, Sattentau QJ. 2004. HIV-1 cell to cell transfer across an Env-induced, actin-dependent synapse. *J. Exp. Med.* 199(2):283–93
107. Hirai M, Takizawa T, Yabuki S, Hirai T, Hayashi K. 1995. Thermotropic phase transition of phosphatidylinositol 4,5-bis(phosphate) aggregates in aqueous solution. *J. Phys. Chem.* 99(48):17456–60
108. Hendrickson HS. 1969. Physical properties and interactions of phosphoinositides. *Ann. N.Y. Acad. Sci.* 165(2):668–76
109. Chakraborty T, Chakraborty I, Ghosh S. 2011. The methods of determination of critical micellar concentrations of the amphiphilic systems in aqueous medium. *Arab. J. Chem.* 4(3):265–70
110. Moens PD, Bagatolli LA. 2007. Profilin binding to sub-micellar concentrations of phosphatidylinositol (4,5) bisphosphate and phosphatidylinositol (3,4,5) trisphosphate. *Biochim. Biophys. Acta Biomembranes* 1768(3):439–49
111. Huang F, Huang K. 1991. Interaction of protein kinase C isozymes with phosphatidylinositol 4,5-bisphosphate. *J. Biol. Chem.* 266(14):8727–33
112. Lee EN, Lee SY, Lee D, Kim J, Paik SR. 2003. Lipid interaction of α-synuclein during the metal-catalyzed oxidation in the presence of Cu^{2+} and H_2O_2. *J. Neurochem.* 84(5):1128–42
113. Palmer FS. 1981. The phosphatidyl-*myo*-inositol-4,5-biphosphate phosphatase from *Crithidia fasciculata*. *Can. J. Biochem.* 59(7):469–76
114. Sugiura Y. 1981. Structure of molecular aggregates of 1-(3-*sn*-phosphatidyl)-L-*myo*-inositol 3,4-bis(phosphate) in water. *Biochim. Biophys. Acta Biomembr.* 641(1):148–59
115. Hendrickson HS, Reinertsen JL. 1969. Comparison of metal-binding properties of *trans*-1,2-cyclohexanediol diphosphate and deacylated phosphoinositides. *Biochemistry* 8(12):4855–58
116. Janmey PA, Iida K, Yin HL, Stossel TP. 1987. Polyphosphoinositide micelles and polyphosphoinositide-containing vesicles dissociate endogenous gelsolin-actin complexes and promote actin assembly from the fast-growing end of actin filaments blocked by gelsolin. *J. Biol. Chem.* 262(25):12228–36
117. Flanagan LA, Cunningham CC, Chen J, Prestwich GD, Kosik KS, Janmey PA. 1997. The structure of divalent cation-induced aggregates of PIP2 and their alteration by gelsolin and tau. *Biophys. J.* 73(3):1440–47
118. Fujita A, Cheng J, Tauchi-Sato K, Takenawa T, Fujimoto T. 2009. A distinct pool of phosphatidylinositol 4,5-bisphosphate in caveolae revealed by a nanoscale labeling technique. *PNAS* 106(23):9256–61
119. Wang J, Richards DA. 2012. Segregation of PIP2 and PIP3 into distinct nanoscale regions within the plasma membrane. *Biol. Open* 1(9):857–62
120. van den Bogaart G, Meyenberg K, Risselada HJ, Amin H, Willig KI, et al. 2011. Membrane protein sequestering by ionic protein-lipid interactions. *Nature* 479(7374):552–55
121. Ji C, Zhang Y, Xu P, Xu T, Lou X. 2015. Nanoscale landscape of phosphoinositides revealed by specific pleckstrin homology (PH) domains using single-molecule superresolution imaging in the plasma membrane. *J. Biol. Chem.* 290(45):26978–93
122. Carvalho K, Ramos L, Roy C, Picart C. 2008. Giant unilamellar vesicles containing phosphatidylinositol(4,5)bisphosphate: characterization and functionality. *Biophys. J.* 95(9):4348–60
123. Honigmann A, van den Bogaart G, Iraheta E, Risselada HJ, Milovanovic D, et al. 2013. Phosphatidylinositol 4,5-bisphosphate clusters act as molecular beacons for vesicle recruitment. *Nat. Struct. Mol. Biol.* 20(6):679–86
124. Myat MM, Anderson S, Allen L-AH, Aderem A. 1997. MARCKS regulates membrane ruffling and cell spreading. *Curr. Biol.* 7(8):611–14
125. Allen L-AH, Aderem A. 1995. A role for MARCKS, the alpha isozyme of protein kinase C and myosin I in zymosan phagocytosis by macrophages. *J. Exp. Med.* 182(3):829–40
126. van Rheenen J, Mulugeta Achame E, Janssen H, Calafat J, Jalink K. 2005. PIP_2 signaling in lipid domains: a critical re-evaluation. *EMBO J.* 24(9):1664–73

127. Milovanovic D, Platen M, Junius M, Diederichsen U, Schaap IAT, et al. 2016. Calcium promotes the formation of syntaxin 1 mesoscale domains through phosphatidylinositol 4,5-bisphosphate. *J. Biol. Chem.* 291(15):7868–76
128. Doughman RL, Firestone AJ, Anderson RA. 2003. Phosphatidylinositol phosphate kinases put PI4,5P_2 in its place. *J. Membr. Biol.* 194(2):77–89
129. van den Bout I, Divecha N. 2009. PIP5K-driven PtdIns(4,5)P_2 synthesis: regulation and cellular functions. *J. Cell Sci.* 122(21):3837–50
130. Nishioka T, Aoki K, Hikake K, Yoshizaki H, Kiyokawa E, Matsuda M. 2008. Rapid turnover rate of phosphoinositides at the front of migrating MDCK cells. *Mol. Biol. Cell* 19(10):4213–23
131. Wen Y, Vogt VM, Feigenson GW. 2018. Multivalent cation-bridged PI(4,5)P_2 clusters form at very low concentrations. *Biophys. J.* 114(11):2630–39
132. Slochower DR, Wang YH, Tourdot RW, Radhakrishnan R, Janmey PA. 2014. Counterion-mediated pattern formation in membranes containing anionic lipids. *Adv. Colloid Interface Sci.* 208:177–88
133. Wang YH, Slochower DR, Janmey PA. 2014. Counterion-mediated cluster formation by polyphosphoinositides. *Chem. Phys. Lipids* 182:38–51
134. Slochower DR, Huwe PJ, Radhakrishnan R, Janmey PA. 2013. Quantum and all-atom molecular dynamics simulations of protonation and divalent ion binding to phosphatidylinositol 4,5-bisphosphate (PIP_2). *J. Phys. Chem. B* 117(28):8322–29
135. Levental I, Cebers A, Janmey PA. 2008. Combined electrostatics and hydrogen bonding determine PIP_2 intermolecular interactions. *J. Am. Chem. Soc.* 130(28):9025–30
136. Hendrickson H, Ballou C. 1964. Ion exchange chromatography of intact brain phosphoinositides on diethylaminoethyl cellulose by gradient salt elution in a mixed solvent system. *J. Biol. Chem.* 239(5):1369–73
137. Fullington JG, Hendrickson HS. 1966. Phospholipid-metal complexes. *J. Biol. Chem.* 241(17):4098–100
138. Hauser H, Dawson RM. 1967. The binding of calcium at lipid-water interfaces. *Eur. J. Biochem.* 1(1):61–69
139. Buckley JT, Hawthorne JN. 1972. Erythrocyte membrane polyphosphoinositide metabolism and the regulation of calcium binding. *J. Biol. Chem.* 247(22):7218–23
140. Levental I, Christian DA, Wang YH, Madara JJ, Discher DE, Janmey PA. 2009. Calcium-dependent lateral organization in phosphatidylinositol 4,5-bisphosphate (PIP2)- and cholesterol-containing monolayers. *Biochemistry* 48(34):8241–48
141. Wang YH, Collins A, Guo L, Smith-Dupont KB, Gai F, et al. 2012. Divalent cation-induced cluster formation by polyphosphoinositides in model membranes. *J. Am. Chem. Soc.* 134(7):3387–95
142. Ellenbroek WG, Wang YH, Christian DA, Discher DE, Janmey PA, Liu AJ. 2011. Divalent cation-dependent formation of electrostatic PIP_2 clusters in lipid monolayers. *Biophys. J.* 101(9):2178–84
143. Sarmento MJ, Coutinho A, Fedorov A, Prieto M, Fernandes F. 2014. Ca^{2+} induces PI(4,5)P_2 clusters on lipid bilayers at physiological PI(4,5)P_2 and Ca^{2+} concentrations. *Biochim. Biophys. Acta Biomembr.* 1838(3):822–30
144. Hansen SD, Huang WY, Lee YK, Bieling P, Christensen SM, Groves JT. 2019. Stochastic geometry sensing and polarization in a lipid kinase-phosphatase competitive reaction. *PNAS* 116(30):15013–22
145. Lagerholm BC, Weinreb GE, Jacobson K, Thompson NL. 2005. Detecting microdomains in intact cell membranes. *Annu. Rev. Phys. Chem.* 56:309–36
146. Golebiewska U, Nyako M, Woturski W, Zaitseva I, McLaughlin S. 2008. Diffusion coefficient of fluorescent phosphatidylinositol 4,5-bisphosphate in the plasma membrane of cells. *Mol. Biol. Cell* 19(4):1663–69
147. Sarmento MJ, Coutinho A, Fedorov A, Prieto M, Fernandes F. 2017. Membrane order is a key regulator of divalent cation-induced clustering of PI(3,5)P_2 and PI(4,5)P_2. *Langmuir* 33(43):12463–77
148. Rodushkin I, Engström E, Baxter DC. 2010. Sources of contamination and remedial strategies in the multi-elemental trace analysis laboratory. *Anal. Bioanal. Chem.* 396(1):365–77
149. Wen Y, Feigenson GW, Vogt VM, Dick RA. 2020. Mechanisms of PI(4,5)P_2 enrichment in HIV-1 viral membranes. *J. Mol. Biol.* 19:5343–64
150. Suh BC, Hille B. 2007. Electrostatic interaction of internal Mg^{2+} with membrane PIP_2 seen with KCNQ K^+ channels. *J. Gen. Physiol.* 130(3):241–56

151. Seo JB, Jung SR, Huang W, Zhang Q, Koh DS. 2015. Charge shielding of PIP_2 by cations regulates enzyme activity of phospholipase C. *PLOS ONE* 10(12):e0144432
152. Wang P, Wang ZY. 2017. Metal ions influx is a double edged sword for the pathogenesis of Alzheimer's disease. *Ageing Res. Rev.* 35:265–90
153. Bilkova E, Pleskot R, Rissanen S, Sun S, Czogalla A, et al. 2017. Calcium directly regulates phosphatidylinositol 4,5-bisphosphate headgroup conformation and recognition. *J. Am. Chem. Soc.* 139(11):4019–24
154. Papayannopoulos V, Co C, Prehoda KE, Snapper S, Taunton J, Lim WA. 2005. A polybasic motif allows N-WASP to act as a sensor of PIP_2 density. *Mol. Cell* 17(2):181–91
155. Xhao H, Michelot A, Koskela EV, Tkach V, Stamou D, et al. 2013. Membrane-sculpting BAR domains generate stable lipid microdomains. *Cell Rep.* 4(6):1213–23
156. Picas L, Viaud J, Schauer K, Vanni S, Hnia K, et al. 2014. BIN1/M-Amphiphysin2 induces clustering of phosphoinositides to recruit its downstream partner dynamin. *Nat. Commun.* 5:5647
157. Zheng J, Cahill SM, Lemmon MA, Fushman D, Schlessinger J, Cowburn D. 1996. Identification of the binding site for acidic phospholipids on the PH domain of dynamin: implications for stimulation of GTPase activity. *J. Mol. Biol.* 255(1):14–21
158. Bethoney KA, King MC, Lemmon MA, Ostap EM, Hinshaw JE. 2009. A possible effector role for the pleckstrin homology (PH) domain of dynamin. *PNAS* 106(32):13359–64
159. Klein DE, Lee A, Frank DW, Marks MS, Lemmon MA. 1998. The pleckstrin homology domains of dynamin isoforms require oligomerization for high affinity phosphoinositide binding. *J. Biol. Chem.* 273(42):27725–33
160. Yandrapalli N, Lubart Q, Tanwar HS, Picart C, Mak J, et al. 2016. Self assembly of HIV-1 Gag protein on lipid membranes generates $PI(4,5)P_2$/cholesterol nanoclusters. *Sci. Rep.* 6:39332
161. Favard C, Chojnacki J, Merida P, Yandrapalli N, Mak J, et al. 2019. HIV-1 Gag specifically restricts $PI(4,5)P_2$ and cholesterol mobility in living cells creating a nanodomain platform for virus assembly. *Sci. Adv.* 5(10):eaaw8651
162. Que EL, Bleher R, Duncan FE, Kong BY, Gleber SC, et al. 2014. Quantitative mapping of zinc fluxes in the mammalian egg reveals the origin of fertilization-induced zinc sparks. *Nat. Chem.* 7(2):130–39